Biological and Clinical Consequences of a *de novo* Mutation in Glutaminase

Amanda Catherine Watts Larson

A dissertation

submitted in partial fulfillment of the

requirements for the degree of

Doctor of Philosophy

University of Washington

2019

Reading Committee:

Mary-Claire King, Chair

Thomas A. Reh

Marshall S. Horwitz

Paul Phillips

Program Authorized to Offer Degree:

Genome Sciences

University of Washington

Abstract

Biological and Clinical Consequences of a *de novo* Mutation in Glutaminase

Amanda Catherine Watts Larson

Chair of the Supervisory Committee:
Professor Mary-Claire King
Department of Genome Sciences

The causes of bipolar disorder have been a mystery for as long as people have been writing about mental illness. Bipolar disorder is clearly familial but is not inherited in a simple way. Genetic studies have implicated genes involved in inhibitory transmission and genes involved in excitatory neurotransmission. In our studies of severe mental illness in patients with no suggestive family history, we identified a damaging *de novo* mutation in *GLS* in a young man with bipolar disorder with psychosis that onset at age 16. *GLS* encodes glutaminase, the enzyme that converts glutamine to glutamate, the excitatory neurotransmitter. Very recently, other mutations in *GLS* have been reported, leading to severe neurological manifestations. The goal of this project was to functionally characterize the patient's *de novo* mutation, GLS p.L606R. I undertook three types of analyses for this purpose. First, I tested activity of purified mutant and wild-type glutaminase proteins. These assays yielded a marginally significantly higher Kcat/Km ratio for the L606R mutant enzyme than for the wildtype enzyme (P = 0.057). Second, I compared the glutamate / glutamine ratios in lymphoblast cells of the patient versus his unaffected parents. The glutamate/glutamine ratio in patient cells was higher than that in comparable cells of his unaffected parents. Third, I compared profiles of >150 metabolites in

lymphoblast cells of the patient to his unaffected parents. Eight metabolites differed significantly between the patient and his parents. The most significant differences were in levels of N-acetyl-aspartyl-glutamate (NAAG) and of glutamine, both elevated in the patient's cells. NAAG is a peptide neurotransmitter that inhibits the release of both inhibitory and excitatory neurotransmitters. The total cellular glutamate (consisting of glutamic acid and NAAG) was significantly elevated in the patient's cells compared to his unaffected parents. Metabolites from several other pathways were also significantly different in the patient. Inosine monophosphate, the first nucleoside produced during purine synthesis, was elevated in the patient. In contrast, the pyrimidine derivative uracil was decreased in the patient. The B-vitamins thiamine (B1) and pantothenate (B5) were both decreased in the patient. Lactate was increased in the patient, potentially caused by the thiamine deficiency. Finally, methionine sulfoxide which is a marker of oxidative stress was increased in the patient. I propose that excess of total cellular glutamate is caused by the increase in glutaminase activity and is modulated by the increase in NAAG and the patient's successful treatment with lithium.

Table of Contents

List of Figures

List of Tables

List of Equations

Acknowledgements

I would like to thank Mary-Claire King for her endless support. My path through graduate school has come with many unique challenges, and Mary-Claire has been with me every step of the way making sure that I don't veer too far off course. It has been a pleasure having an advisor who is so passionate about what she does and the people she surrounds herself with. I would also like to thank my committee, Tom Reh, Paul Phillips and Marshall Horwitz for their advice, support and thought-provoking conversations.

Thank you to current and past members of the King Lab for encouragement, technical support and friendship. I give special thanks to Tom Walsh, Silvia Casadei, Sarah Pierce, Hannah Kortbawi, Chris Pennil and Anna Sunshine.

I would like to acknowledge my academic department, Genome Sciences, especially Brian Giebel for all he does for the graduate students.

Many friends have supported me and followed my adventures as I traversed the country. I would like to specifically thank Christina Ramirez, Michelle Dunning, Cailyn Spurrell and Stephanie Battle. Their advice, encouragement and shenanigans have helped me get through difficult times and stay sane during graduate school.

I want to thank my family for all of their support and encouragement throughout the years. I give very special thanks to Rowan, who has been the only constant in my life for the last 12 years. It has been an honor having you in my life.

I would like to dedicate this thesis to my mother, Vicky, and my grandmother, Phyllis. They were strong, smart and beautiful women that I am fortunate to have looked up to. I know they would be incredibly proud of me. I love and miss you both.

Chapter 1: Introduction

1.1 Background of Bipolar Disorder

1.1.1 Clinical features

Bipolar disorder (BD) is a severe mental illness that causes significant disability and economic burden. The lifetime risk of BD is approximately 1.0-1.5% worldwide, with males and females affected with equal frequency. Symptoms typically present in late adolescence to early adulthood.

Bipolar disorder, previously termed manic-depressive illness, manifests with extreme fluctuations in mood, energy and activity levels. Both manic and depressive states can last from weeks to months, and it is possible to have a mood episode with mixed features. In between episodes there is typically complete absence of symptoms. There are several subtypes of BD: type I, which consists of full manic episodes; type II, which involves depression and hypomania (a milder form of mania); and bipolar with schizoaffective disorder, which includes psychotic symptoms accompanying manic episodes. Psychotic symptoms are common in BD, with up to 90% of affected individuals experiencing at least one psychotic episode in their lifetime.[1] Individuals presenting with psychotic symptoms at first admission may be initially diagnosed on the schizophrenia spectrum (e.g. schizoaffective disorder), and it is common for the illness to stabilize only after 24 months or so.[2]

The first line therapy for BD depends on the phase of illness the patient is experiencing at presentation, and if the patient is already on treatment. For patients not already on medication who are experiencing mania or a mixed episode, pharmacotherapy consists of a mood stabilizer (e.g. lithium or valproate) alone or in combination with an antipsychotic. For treatment-naïve patients presenting with bipolar depression, an antidepressant may be prescribed in addition to the mono- or combination therapy.

1.1.2 Genetics

Family, twin, and adoption studies revealed a strong genetic component to BD. A study of 30 pairs of monozygotic twins and 37 pairs of dizygotic twins from the United Kingdom estimated the heritability of BD to be between 85% for narrowly-defined BD (i.e. a co-twin had both manic and depressive episodes) and 89% when the criteria was relaxed to include unipolar depression.[3] The lifetime risk for BD in the general population is 0.5-1.5%; however first-degree relatives of a proband with BD have a 5-10% lifetime risk, and monozygotic twins of a proband with BD have a 40-70% lifetime risk. First-degree relatives of a proband with BD also have increased risk of unipolar depression, greater than the risk for BD.[4,5] Despite its high heritability, classical genetic approaches such as linkage analysis, candidate gene and genome wide association studies have not solved the genetics of the disorder.

As genomic technology improved, rare copy number variants (CNVs) and point mutations with large effect size have emerged as promising avenues of dissecting the genetics of BD. Copy number variation has been demonstrated to be an important genetic mechanism in schizophrenia, autism, and mental retardation[6], but evidence on the role of CNVs in BD is less consistent. Several large case-control studies found no enrichment for CNVs in patients with BD.[7,8,9,10,11,12] In contrast, Malhotra et al. found an enrichment for *de novo* CNVs in a cohort of 185 BD trios, and Zhang et al. identified an increase in singleton (i.e. ultra-rare) CNVs in a cohort of 1001 cases and 1033 controls.[13,14] There is also evidence that CNVs are enriched when diagnosis is at an early age of onset, either ≤ 18 years old[13] or ≤ 21 years old[15] or for schizoaffective disorder[10]. Contradictory results of CNV studies may be due to differences in diagnostic criteria for BD, in genomic technology for identifying CNVs, or in filtering strategies that define CNV size and frequency in the population. There is general agreement that CNVs play less of a role in BD than in schizophrenia, autism, or mental retardation.

Ultra-rare and *de novo* point mutations are also well-established to play a role in psychiatric disorders such as autism spectrum disorder and schizophrenia. To investigate the

role of rare mutations in BD, Ament et al. sequenced whole genomes of 200 individuals from 41 pedigrees with multiple affected individuals, and of 254 controls.[16] They first analyzed 2511 genes involved in synaptic or neuronal function, and 669 genes within 100kb of previously identified single nucleotide polymorphisms (SNPs) from genome-wide association studies of BD. Based on the most promising variants in this analysis, they carried out targeted sequencing of the coding and regulatory regions of 26 genes in an independent series of 3014 BD cases and 1717 controls. No single gene carried significantly more coding mutations in cases than controls. However, individually rare noncoding mutations in promoters and enhancers were significantly enriched in affected individuals, specifically in genes involved in neuronal excitability, including $GABA_A$ receptors and voltage-gated calcium channels.

To further elucidate the role of rare and *de novo* variants for BD, Kataoka et al. sequenced the exomes of 56 trios of probands with BD Type I and 23 trios of probands with BD Type II.[17] *De novo* point mutations were significantly more frequent in patients with younger age of onset, similar to the results of studies of *de novo* CNVs.[13,15] Pathways particularly likely to harbor *de novo* damaging mutations were those involving calcium-ion binding, serine-type peptidase activity and serine hydrolase activity.

In summary, genetic studies are beginning to reveal that many individually ultra-rare, private or *de novo* damaging variants will explain the manifestation of BD in some patients. Studies that include detailed clinical findings of affected individuals will help to specify the relationships between clinical phenotypes and the genes and pathways harboring these mutations. So far calcium-ion binding, voltage-gated calcium channels, and inhibitory neurotransmission are emerging as important neurobiological mechanisms in BD supported by genetic data.

1.1.3 Glutamate in bipolar disorder

Glutamate is the main excitatory neurotransmitter in the central nervous system and has been studied extensively in the context of neurological and psychiatric disorders. Several studies have sought to identify differences in the glutamatergic pathway in affected individuals compared to controls using post-mortem brain tissue. Levels of glutamate were increased in the frontal cortex of patients with BD compared to individuals with schizophrenia or controls.[18] Transcription of the glutamate transporter *VGLUT1* was also increased in the anterior cingulate cortex of individuals with BD compared to controls.[19] The authors hypothesized that these findings indicated increased in glutamatergic neurotransmission in BD.

Additional evidence for a role for the glutamatergic pathway in the pathophysiology of BD is based on the mechanism of action of lithium, the first-line therapy for BD that is especially effective at long-term mood stabilization and reducing suicide risk. A study of cerebrocortical slices and synaptosomes from mice found that glutamate uptake was inhibited with treatment of lithium. There was initially a wide range of glutamate uptake in synaptosomes of individual mice, but long-term treatment with lithium stabilized glutamate uptake in synaptosomes thereby reducing variability.[20] The results of these analyses along with the new evidence from genetic studies support the significance of glutamatergic neurotransmission in BD.

1.2 Glutaminase Structure and Function

1.2.1 Gene and protein structure

Two genes code for mammalian glutaminases (GLS; Enzyme Commission 3.5.1.2): *GLS* (or *GLS1)* on chromosome 2q32.3 and *GLS2* on chromosome 12q13.3. The two genes encode four main isoforms. Kidney-type isoforms KGA and GAC are alternatively spliced in a tissue-specific manner from *GLS1*. Liver-type isoforms LGA and GAB are derived from alternative transcription initiation sites of *GLS2*.

The KGA and GAC isoforms contain a mitochondrial localization signal, EF-hand-like and glutaminase domains. KGA contains three ankyrin repeat domains and a kinase extension nuclease domain (Figure 1.1), whereas GAC contains a short unstructured C-terminal domain.

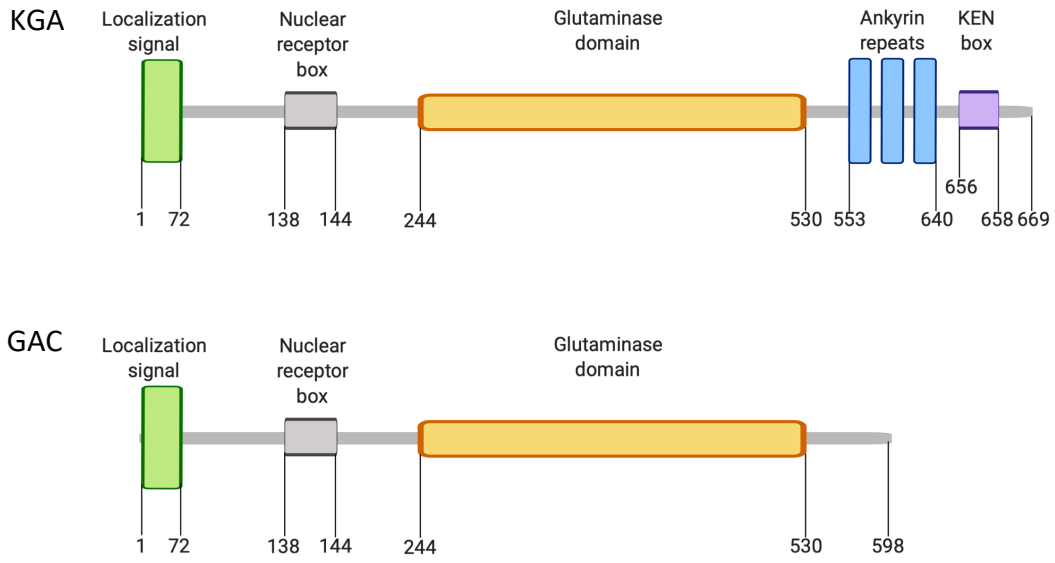

***Figure 1.1*. The protein domain architecture of KGA and GAC isoforms of glutaminase, both encoded by *GLS*.** Both KGA and GAC have a mitochondrial localization signal, a nuclear receptor box, and the catalytic glutaminase domain. The C-terminus of KGA contains three ankyrin repeat domains and a KEN-box, while GAC has a shorter and unstructured C-terminus.

Ankyrin repeat domains are typically involved in protein interactions. However, X-ray crystallography of the KGA C-terminal region revealed that its ankyrin repeats mediate the formation of homo-oligomers.[21] This uncharacteristic interaction has important consequences for the higher order structure of the protein, as well as for the activity of the enzyme. Ferreira et al. determined that the absence of a structured C-terminal domain permits the GAC isoform to organize into a "supra-tetrameric oligomer," whereby the protein forms long rod-like filaments.[22] Both KGA and GAC form these filaments upon activation with inorganic phosphate, but GAC filaments are more than twice as long as the KGA equivalent.[22] Longer filament size is associated with increased catalytic activity of the enzyme.[22]

1.2.2 Expression and regulation

The four isoforms of glutaminase (KGA, GAC, LGA and GAB) all contain an N-terminal mitochondrial localization signal, and GAC and GAB are found exclusively in the mitochondria. Both KGA and LGA are present in the cytosol and nuclei, but in brain tissue KGA is localized to the mitochondria while LGA is confined to the nuclei.[23] KGA and LGA have similar expression patterns throughout the brain and are most highly expressed in the cerebral cortex with lowest expression in the spinal cord and medulla.[23] KGA and GAC were both up-regulated throughout neuronal differentiation from primary human neuronal progenitor cells.[24]

Regulation of *GLS* has been studied primarily in the context of carcinogenesis and HIV-associated neurocognitive disorders. By serial deletion of the *GLS* promoter and mutational-screening of eight STAT1 binding sites within that region, Zhao et al identified two STAT1 binding sites that led to increased or decreased *GLS* expression in monocyte-derived macrophages.[25] In mouse embryonic fibroblasts, the induction of Myc led to increased expression of *GLS* and an increase in glutamine uptake.[26] During carcinogenesis, microRNAs miR-23a and miR-137 inhibit *GLS* transcription.[27,28] Interestingly, both of these microRNAs have been shown to be important for neuronal and glial cell function, and variants within them have been associated with neuropsychiatric disorders.[29]

The glutaminase protein is activated by inorganic phosphate (P*i*) and is inhibited by the products of its reaction, glutamate and NH_3.[30] Calcium activates glutaminase from synaptosomes isolated from rat brain but does not activate purified glutaminase, indicating that the regulatory effect is indirect.[30] Cassago et al. established that P*i* activates glutaminase by opening a gating loop at amino acid residues 321-LRFNKL-326 that competes with glutamate and facilitates the formation of the supra-tetrameric filaments.[31]

1.2.3 Functions of glutaminase

Glutaminase is an amidohydrolase that converts glutamine to glutamate (Figure 1.2). Glutamate is as a source of energy in cellular metabolism, a direct intermediary of α-ketoglutarate via glutamate dehydrogenase for TCA cycle anaplerosis, a downstream metabolite of the antioxidant glutathione, and a provider of nitrogen for lipid and protein synthesis. Importantly, glutamate also serves as the key excitatory neurotransmitter. In the central nervous system, glutamine is transported from astrocytes to pre-synaptic neurons where it is converted to glutamate by glutaminase (Figure 1.3).

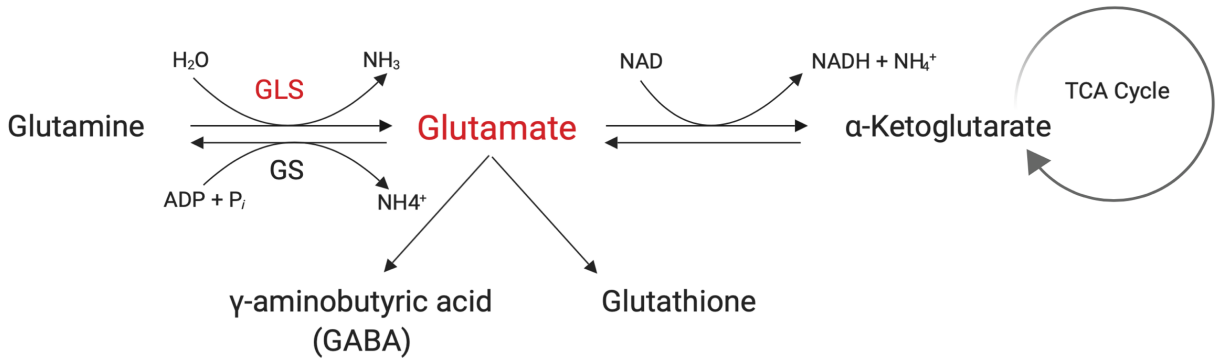

***Figure 1.2*. Glutamate pathways**.
Glutaminase catalyzes the reaction: L-glutamine +H_2O -> L-glutamate + NH_3. Glutamate is also synthesized from α-ketoglutarate via a transaminase reaction (not shown in figure). Glutamate can be further processed into the neurotransmitter GABA or the antioxidant glutathione.

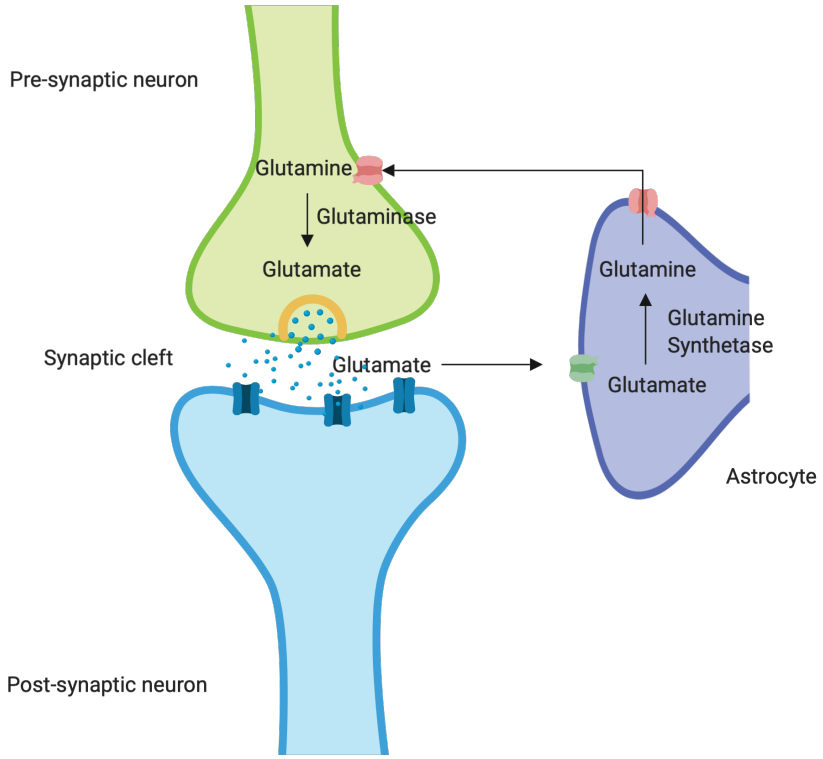

Figure 1.3. **Glutamate recycling in the CNS.**
Glutamate that has been released into the synaptic cleft is transported into astrocytes where it is converted into glutamine by glutamine synthetase. It is then shuttled back to the pre-synaptic neuron where glutaminase converts it back to glutamate and it can be packaged into synaptic vesicles for release.

While the role of *GLS* in mature neurons is well-established, the function of *GLS* during neurodevelopment remained unknown. To address this, Wang et al. used siRNA to knock down *GLS* expression in human primary neural progenitor cells (NPCs), then differentiated the NPCs into neurons.[24] They found that *GLS* was important for several key aspects of neurodevelopment, including NPC proliferation and maintenance, and neuronal differentiation.

1.3 Glutaminase and Neurological Disorders

1.3.1 Glutaminase mutations in neurological disorders

Altered glutamate metabolism via dysregulated glutaminase has been described in several neurological disorders[32,33,34,35,36,37], but human disease-causing mutations of *GLS* were first reported in 2018.[38] Within a year, three additional reports of mutations were published making *GLS* an emerging disease gene outside of its previously known dysregulation.[39,40,41]

Disease-causing mutations have also been described for other genes directly involved with glutamate metabolism. Glutamine synthetase deficiency is a rare recessive inborn error of metabolism with a severe manifestation leading to early death. Children with the disorder suffer from encephalopathy, multiple organ failure, seizures, and respiratory failure. The longest-lived patient was treated with glutamine supplementation but died at six years old.[42,43]

Inborn errors of metabolism are typically caused by loss of function mutations which lead to deficiency of an enzyme, as illustrated above. In contrast, activating mutations in glutamate dehydrogenase cause hyperinsulinism-hyperammonemia syndrome. Patients with this disorder present have hypoglycemia and a high incidence of seizures.[44]

Interestingly, both loss of function and gain of function mutations have been described in *GLS* (Table 1.1). The first loss of function mutations were described in individuals with spastic ataxia and optic atrophy.[38] Two brothers shared a homozygous duplication of *GLS* exon 1, leading to complete loss of *GLS* expression.[38] The brothers were unaffected until age 7 years, then developed motor and gait issues, and within a year began to lose vision due to optic atrophy. The illness was progressive and both patients were wheelchair-bound when last described at ages 27 and 30 years.

Table 1.1 **Clinical features and mutation information of patients with *GLS* mutations**
Mutations at c.-212 are expansions of a GCA repeat [with the number of repeats indicated in brackets]

Clinical features	Genomic position (hg19)	cDNA change	Protein change	Inheritance	Age of onset
Spastic ataxia and optic atrophy[38]	Chr2:191,750,021-Chr2:191,742,079		n/a	Recessive	7 y
Epileptic encephalopathy (2 siblings)[39]	Chr2:191,765,378	c.695dup	D232Efs*2	Recessive (homozygous)	Neonatal
Epileptic encephalopathy (2 siblings)[39]	Chr2:191,746,051 Chr2:191,766,752	c.241C>T c.815G>A	Q81* R272K	Recessive (compound het)	Neonatal
Developmental delay and ataxia[40]	Chr2: 191,745,599 Chr2: 191,769,852	c.-212GCA[680] c.938C>T	n/a P313L	Recessive (compound het)	3 y
Developmental delay and ataxia[40]	Chr2: 191,745,599	c.-212GCA[900] c.-212GCA[1400]	n/a n/a	Recessive (compound het)	3 y
Developmental delay and ataxia[40]	Chr2: 191,745,599 Chr2: 191,769,837	c.-212GCA[1500] c.923dupA	n/a Y308*	Recessive (compound het)	2 y
Developmental delay and bilateral cataracts[41]	Chr2:191,795,182	c.1445C>G	S482C	*de novo* (heterozygous)	3 mo

Rumping et al. described bi-allelic loss of function variants in three infants from two families with refractory epileptic encephalopathy and respiratory insufficiency.[39] The affected child in one family was homozygous for a frameshift mutation, and the two infants in the second family were compound heterozygous for a nonsense and putatively damaging missense mutation. Mass spectrometry of protein extracted from blood spots of the affected children and unaffected children born on the same day revealed increased levels of glutamine, but not of glutamate, in blood from affected infants.

Very recently, a repeat expansion in the *GLS* 5' untranslated region was discovered in children from three families who presented at ages 2-3 years with motor and speech delay, progressive ataxia, and increased plasma glutamine.[40] One affected child was heterozygous for a missense mutation and a repeat expansion, one child was homozygous for large repeat expansions, and the third child was heterozygous for a large repeat expansion and a nonsense

mutation (Table 1.1). Patient fibroblasts had decreased levels of glutamate, and recombinant proteins carrying the point mutations had little to no enzymatic activity. Expansion of the 5'UTR (GCA)-repeat resulted in reduced expression of *GLS*, perhaps due to a decrease in activating histone marks in patient fibroblasts compared to controls.

The first report of a *de novo* activating mutation in *GLS* was in a child with profound developmental delay and infantile cataract.[41] Mass spectrometry of fibroblasts revealed an increased glutamate/glutamine ratio compared to controls, indicating the mutant glutaminase was hyperactive. This result was repeated when the patient's mutation was overexpressed in HEK293T cells. When CB-839, a potent glutaminase inhibitor was applied to the cells expressing the mutation, the glutamate/glutamine ratio normalized.

In our lab, exome sequencing of 21 proband-parent-parent trios and 84 proband-sibling-parent-parent quads revealed in one proband identified a *de novo* mutation in *GLS*.[45] The characterization of this mutation is the subject of this dissertation.

The recent surge in identification of disease-causing mutations in *GLS* implicates dysregulated glutamate metabolism in central nervous system disorders including ataxia, respiratory insufficiency, developmental delay, and epileptic encephalopathy. The mutations cover a wide range of mechanisms from missense to repeat expansion and can result in both loss of function and gain of function. In mice, complete loss of glutaminase function resulted in respiratory-induced death on postnatal day 1.[46] The human allele with the most severe loss of function also leads to neonatal mortality.[39] The other reported human alleles likely retain some function, with patients surviving past age 20 years.

1.4 Scope of Thesis

The goal of this project was to determine the functional consequences of a damaging *de novo* mutation identified in a patient with BD with psychosis. Genetic studies are creating the framework for elucidating potential pathways involved in the molecular mechanisms of BD.

Excitatory neurotransmission via the glutamatergic pathway has been implicated in the pathophysiology of BD by genetic, post-mortem, and therapy-based studies.

Based on the structure and function of glutaminase, I hypothesized that the mutation of this patient resulted in a hyperactive protein that impacts metabolic pathways. My observations from an *in vitro* enzyme assay supported this hypothesis. Furthermore, analysis of lymphoblast cell lines from the patient and his parents for >150 metabolites revealed that levels of glutamate and the peptide neurotransmitter N-acetyl-aspartyl-glutamate were significantly increased in the patient's cells.

Chapter 2: Functional characterization of *de novo* mutation in glutaminase

2.1 Clinical features and gene discovery

2.1.1 Clinical features

The patient is a Caucasian male who presented at the Children's Study Center of Western Washington State Hospital at age 16 with acute changes in mood, thoughts, and sleep patterns. Neither he nor his parents had a prior history of mental illness and prior to this episode he had normal developmental milestones. Due to his mixture of manic and psychotic features he was originally diagnosed with schizoaffective disorder, however over the course of two years his symptoms stabilized, and he was re-diagnosed with bipolar disorder with psychosis. The patient responded well to treatment with lithium.

2.1.2 Gene discovery

Genomic DNA was extracted from peripheral blood, and whole exome sequencing was performed on the patient and his unaffected parents using NimbleGen SeqCap EZ Library v2.0 (Roche, Basel, Switzerland). Variants were filtered to identify those that were both *de novo* in the patient and predicted to be damaging to the protein product. Only one variant of the patient fit these criteria, missense mutation *GLS* c.1817T>G, p.Leu606Arg (NM_014905.4) at chr2:191,819,508 (hg19). Sanger sequencing confirmed the variant to be heterozygous in the patient and absent in both unaffected parents. This mutation has not been reported in >125,000 exomes and whole genome sequences in gnomAD[47] or in our in-house database.

GLS is intolerant to missense mutations (gnomAD missense Z score = 3.73). GLS L606R was predicted to be damaging to the protein product by *in silico* prediction tools: PolyPhen-2 score 0.992; SIFT P= 0.001; CADD score 25.5.

2.2 Materials and Methods

2.2.1 Subjects

Informed consent was obtained from all study subjects according to protocols approved by the Institutional Review Boards at the University of Washington and Seattle Children's Hospital.

2.2.2 Generation of constructs

The wild type human *GLS* open reading frame in the pCMV6-entry vector was obtained from OriGene Technologies, Inc. (catalog #RC206265, Rockville, MD). The wild type KGA Val124-Leu669 (WT) construct, with an N-terminal His6 tag, was produced by amplifying the appropriate region of the *GLS* ORF by PCR and subcloning into the pET-28a(+) protein expression vector using NheI and SalI restriction sites. Glutaminase mutations L606R, R272K and S482C were created using the Q5 Site-Directed Mutagenesis Kit (catalog #E0554S, New England Biolabs, Ipswich, MA).

2.2.3 Protein purification

The WT and three mutant constructs were transformed into *Escherichia coli* Rosetta2(DE3)pLysS competent cells (catalog #71403, MilliporeSigma, Burlington, MA). Overnight cultures were grown at 37°C shaking at 200 rpm in LB medium supplemented with 50 μg ml^{-1} kanamycin and 50 μg ml^{-1} cloramphenicol. The overnight cultures were then diluted 1:100 in a total volume of 200 ml and grown at 37°C until the OD600 reading was between 0.6 and 0.8. The temperature was then reduced to 18°C for at least 30 minutes before protein expression was induced with 250 μM isopropyl β-D-1-thiogalactopyranoside (IPTG), and cultures were grown overnight at 18°C. Bacteria were centrifuged at 4,000rpm for 15 minutes and supernatant was drained. Twenty mL of BugBuster Protein Extraction Reagent (catalog

#70584, MilliporeSigma, Burlington, MA) was supplemented with 2 Pierce EDTA-free protease inhibitor tablets (catalog #A32965, ThermoFisher, Waltham, MA), 10 mM imidazole and 250 U/mL benzonase, and the bacterial cell pellets were resuspended in 5 ml of the prepared lysis buffer per 1 mg of pellet, then centrifuged at 16,000xg for 20 min at 4°C. Supernatant was then filtered with 0.45 µM syringe filter into 15 ml Falcon tubes.

KGA protein variants were purified using His60 Nickel Gravity Columns (catalog #635658, Takara Bio, Inc., Mountain View, CA). Nickel columns were washed twice with equilibration buffer (25 mM Tris pH 8.5, 500 mM NaCl, 20 mM imidazole), then 5 ml of protein extract was added to the column and rotated for one hour at 4°C. The column was washed twice with equilibration buffer, then twice with wash buffer (25 mM Tris pH 8.5, 500 mM NaCl, 50 mM imidazole). Purified protein was eluted in ten-1 mL aliquots using elution buffer (25 mM Tris pH 8.5, 200 mM NaCl, 300 mM imidazole). All ten fractions were analyzed on a Coomassie blue-stained SDS-PAGE gel, and fractions with the highest proportion of anticipated product size were pooled for dialysis. Pooled fractions were dialyzed overnight at 4°C in dialysis buffer (30 mM Tris pH 8.5, 150 mM NaCl, 0.5 mM Tris(2-carboxyethyl)phosphine. Aliquots of purified protein were flash frozen in liquid nitrogen and stored at -80°C.

2.2.4 Glutaminase assay

A coupled reaction adapted from Pasqualli et al was used to determine the catalytic activity of the four KGA proteins.21 Reactions included purified protein at 10nM, 3 U L-glutamic dehydrogenase (catalog #G2626, Sigma Aldrich, St. Louis, MO), 2mM β-Nicotinamide adenine dinucleotide hydrate (NAD; catalog # N1636, Sigma Aldrich, St. Louis, MO) and 50mM Tris-acetate, pH 8.6. Potassium phosphate (K_2HPO_4, stock 2M, pH 9.4) was added in concentrations from 0-50 mM. The mixture containing purified protein, L-glutamic dehydrogenase, NAD, Tris-acetate and potassium phosphate was added to 96-well plates pre-filled with serial dilutions of L-glutamine for a range of concentrations between 0-40 mM. The final volume of the reaction

was 200 µl. The formation of NADH was measured at an absorbance of 340 nm over 5 min at room temperature. Readings were taken on a Synergy HT1 Hybrid Multi-Mode Plate Reader (BioTek, Winooski, VT).

Initial velocities in picomoles of NADH produced per second were calculated by first determining the slope of each reaction, then using the Beer-Lambert Law (Absorbance = ε L c, where ε is the extinction coefficient for NADH, L is the pathlength, and c is the solution concentration in mol/L). I used the extinction coefficient for NADH of 6220 M^{-1} cm^{-1} and a pathlength of 0.5 cm. All measurements were done in triplicate, and analyzed using GraphPad Prism 8.1.2 (GraphPad Software, San Diego, CA).

Next, I sought to determine the full kinetic profile of each enzyme by calculating V_{max}, K_m, and K_{cat}. V_{max} is the maximal rate of the reaction. The Michaelis-Menten constant, K_m, is the substrate concentration at which the enzyme functions at half of V_{max} and can be viewed as the binding affinity of the enzyme to its substrate. A lower K_m value indicates a higher binding affinity to the substrate, as the enzyme requires less substrate to reach V_{max} to more quickly. K_{cat} is the turnover rate of the enzyme, or the number of substrate molecules that an enzyme catalytic site converts to product per unit time. K_m is derived from the general enzyme reaction equation as shown in Equation 1.1.

$$E + S \underset{k_{-1}}{\overset{k_1}{\leftrightarrow}} ES \overset{k_2}{\rightarrow} E + P \quad (1.1a)$$

$$ES = k_1 [E][S] \quad (1.1b)$$

$$ES = (k_{-1} + k_2)[ES] \quad (1.1c)$$

$$k_1 [E][S] = (k_{-1} + k_2)[ES] \quad (1.1d)$$

$$[\mathrm{E}][\mathrm{S}]/[\mathrm{ES}] = (\mathrm{k}_{-1} + \mathrm{k}_2)/\mathrm{k}_1 \quad (1.1e)$$

$$\mathrm{K_m} = [\mathrm{E}][\mathrm{S}]/[\mathrm{ES}] \quad (1.1f)$$

Equation 1.1. **Derivation of the Michaelis Constant, K_m.**
1.1a is the enzyme reaction equation where E is enzyme, S is substrate and P is product. 1.1b is the rate of formation of the enzyme-substrate complex. Brackets indicate concentration. 1.1c is the breakdown of the enzyme-substrate complex. Equation 1.1d is the equations 1.1b and 1.1c set equal to each other because we are assuming a steady state intermediate. Equation 1.1e rearranges equation 1.1c so the initial enzyme and substrate concentrations divided by the enzyme-substrate complex is equal to the rate of breakdown of the complex plus formation of product divided by the formation of the complex. This is considered the Michaelis Constant, K_m as shown in equation 1.1f.

The Michaelis-Menten equation combines V_{max}, K_m and the substrate concentration and is shown in Equation 1.2. The Michaelis-Menten model can be illustrated as shown in Figure 2.1. Finally, K_{cat}, the enzyme turnover, takes into account both the maximal rate of reaction, Vmax, and the total enzyme concentration [ET] and is calculated as V_{max}/[ET].

$$V = V_{max}\left(\frac{[S]}{[S] + K_m}\right) \quad (1.2)$$

Equation 1.2. **Michaelis-Menten Equation.**
The velocity is the reaction rate at a substrate concentration. It is equal to the maximal rate of the reaction multiplied by the substrate concentration divided by the substrate concentration plus the Michaelis constant, K_m, derived as described as above. Units of this equation are reported as concentration per second.

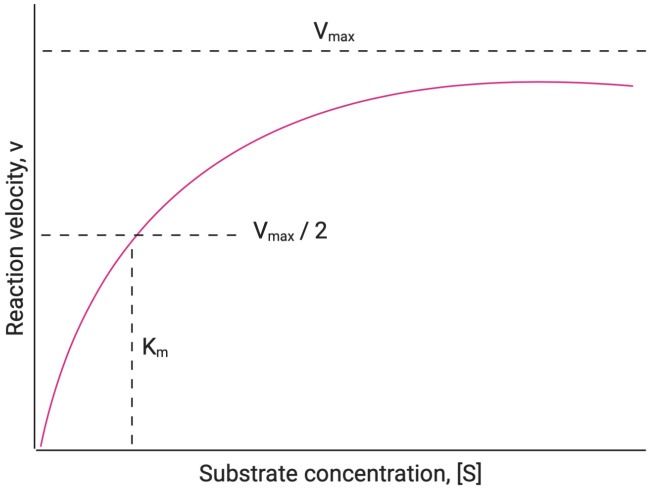

Figure 2.1. **Michaelis-Menten Model.**
V_{max} is the fastest rate the enzyme can act on the substrate. K_m is the substrate concentration at which the enzyme is working half as fast as it can ($V_{max}/2$).

The mathematical model provided by GraphPad Prism 8.1.2 to calculate V_{max} and K_m is: $Y = V_{max} * X / (K_m + X)$, where Y is the enzyme velocity (v_0 as calculated by the slope of the line) and X is the substrate concentration. To calculate K_{cat}, the GraphPad Prism model is $Y = Et * K_{cat} * X(K_m + X)$, where Y is the enzyme velocity (V_0), X is substrate concentration and Et is the concentration of enzyme catalytic sites.

2.2.5 Mass spectrometry

Lymphoblast cell lines from the proband and his unaffected parents were grown in RPMI1640 media supplemented with 15% fetal bovine serum, 2 mM L-glutamine, and 1X penicillin/streptomycin 10,000 U/ml. Cells were seeded at $0.3x10^5$ per T25 flask, then harvested three days later so they would be at a similar growth phase. Cells were washed twice with ice cold PBS, and $1x10^6$ cells were aliquoted into Eppendorf tubes, flash frozen with liquid nitrogen then stored at -80°C. Cells were grown independently twice and quadruplicate aliquots of each were analyzed.

Samples were transported on dry ice to the University of Washington Northwest Metabolomics Research Center for analysis. Targeted aqueous metabolite profiling analysis was performed using hydrophilic interaction chromatography (HILIC) with a Sciex 6500+ LC-MS/MS instrument using standard operating procedures.[48] To monitor sample preparation and system performance, four isotype labeled internal standards were included, and quality control samples were included at the start of the run and after every 10 samples. Data were integrated in Sciex-OS v1.5. The data was normalized to log-transformed total ion current and analyzed with GraphPad Prism 8.1.2.

2.2.6 Statistics

For analysis of glutaminase activity, the assay was carried out three times independently for the wild-type and three mutant enzymes on different days, with each assay on each day including three technical replicates. To evaluate Michaelis-Menten parameters, average values of technical replicates for each of the three mutant enzymes were compared to the wild-type enzyme using paired t-tests.

For analysis of metabolite profiles, four technical replicates of cells of the proband and four of each of his parents were tested. For each metabolite, values of the proband were compared to the values of both parents (8-replicates) using unmatched t-tests. P-values were corrected by the Bonferroni method for multiple comparisons: 75 tests for metabolites evaluated in positive ion mode and 80 tests for metabolites evaluated in negative ion mode.

2.2.7 Generation and maintenance of induced pluripotent stem cells

Lymphoblast cells from the proband and his unaffected parents were maintained as above. The protocol for reprogramming lymphoblast cells was adapted from Thomas et al.[49] On day 0, $2x10^6$ cells were transfected with 2 µg each of the following episomal vectors: pCXLE-hOCT3/4-shp53-F, pCXLE-hSK, pCXLE-hUL, and pCXLE-EGFP (Addgene IDs: 27077, 27078,

27080 and 27082, respectively; all gifts from Shinya Yamanaka) using the Amaxa nucleofector program X-005 (Lonza Group, Basel, Switzerland). Cells were then plated in a 12-well plate, and media (WiCell supplemented with 50 µg/ml vitamin C and 0.5 mM sodium butyrate) was changed every other day until day 8. On day 3 cells were inspected for expression of GFP. On day 8 the transfected lymphoblast cells were transferred to 6-well plates previously coated with mouse embryonic fibroblasts (a kind gift from Sergei Doulatov, University of Washington). On day 12 sodium butyrate was removed from the media, and media was replaced every other day. Between days 16-18 pluripotent stem cell colonies began forming, and by day 24 colonies were passaged.

After passage 3, the induced pluripotent stem cell (iPSC) lines were transitioned from mouse embryonic fibroblasts to human embryonic stem cell-qualified LDEV-free Matrigel (catalog #354277, Corning, Corning, NY), and media was changed to mTeSR1 (catalog #85850, STEMCELL Technologies, Vancouver, BC) supplemented with 1X penicillin/streptomycin. Colonies were passaged on a 7-day passaging protocol using ReLeSR (catalog #05872, STEMCELL Technologies, Vancouver, BC). Three separate colonies were clonally expanded for each line and banked in liquid nitrogen.

2.2.8 Validation of pluripotent status and genomic integrity of iPSCs

Immunofluorescence of the pluripotency marker OCT4 was used to confirm the pluripotency of the iPSC lines. Colonies were plated on Matrigel-coated Lab-Tek chambered cover glass slides (catalog #155383PK, ThermoFisher, Waltham, MA). The colonies were washed twice with PBS and fixed in 4% paraformaldehyde for 10 min, then incubated for one hour at room temperature in PBS with 10% normal horse serum and 0.5% Triton X-100 to block non-specific protein-protein interactions. The OCT4 antibody (1:1000 dilution, catalog #ab109884, Abcam, Cambridge, UK) was added and slides were incubated overnight at 4°C. Slides were washed five times with PBS, then incubated in secondary antibody labeled with

Alexa Fluor 488 (1:500, catalog #ab150073, Abcam, Cambridge, UK) in the dark for one hour at room temperature. Slides were washed five times in PBS and nuclei were stained using Fluoroshield mounting medium with DAPI (catalog #ab104139, Abcam, Cambridge, UK).

2.2.9 Glutamate/Glutamine-Glo Assay in iPSCs

The "Glutamate/Glutamine Glo Assay" (catalog #J8021, Promega Corporation, Madison, WI) was used to study the levels of glutamate and glutamine in the iPSC lines. iPSC colonies were dissociated into single cells using Gentle Cell Dissociation Reagent (catalog #07174, STEMCELL Technologies) and counted. Cells were washed twice in ice cold PBS, then aliquoted into Eppendorf tubes and stored at -80°C. A pilot study was conducted with 5,000, 10,000, 20,000 and 40,000 cells to determine the linear range of the assay. The kit protocol was followed using 20,000 cells with four technical replicates. Due to lack of sufficient cells to repeat the experiment, only one experimental replicate was performed. Luminescence was read using the Synergy H1 Hybrid Multi-Mode Microplate Reader (BioTek, Winooski, VT).

2.3 Results

2.3.1 Kinetic parameters of wild type and mutant glutaminase

The KGA and GAC isoforms of glutaminase differ in C-terminal structure, as indicated in Figure 1.2. KGA contains three ankyrin repeats and GAC has a truncated and unstructured C-terminus. Pasqualli et al. determined that the absence of ankyrin repeats was responsible for the higher enzymatic activity of the GAC isoform, and that this increased activity was likely due to the ability of the GAC isoform to form long filaments.[21]

The L606R mutation lies in an ankyrin repeat of the KGA isoform. I hypothesized that this mutation could result in a more active enzyme than wild type, potentially by slightly altering the ankyrin repeat dimer enough to allow longer filaments to form.

To test the hypothesis that the L606R mutation results in a more active enzyme, I created recombinant human glutaminase and tested its activity in an assay adapted from Cassago et al.[31] In addition to L606R, we also created R272K, a loss-of-function mutation identified in a neonate with epileptic encephalopathy[39], and S482C, an activating mutation identified in an infant with profound developmental delay[41]. The mutations are described in Table 1.1 and their locations in the protein are illustrated in Figure 2.2. To my knowledge, enzyme activity has not been previously reported for any of these mutations.

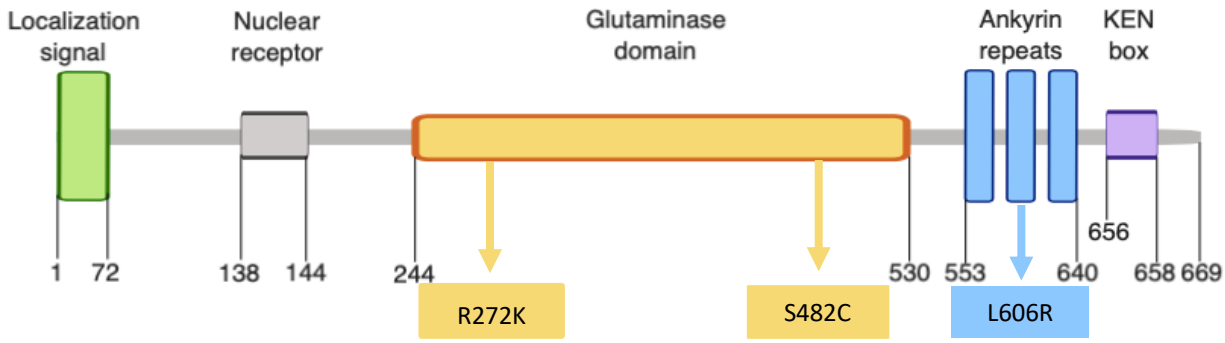

Figure 2.2 **Missense mutations in the glutaminase protein.**

The glutaminase enzyme assay is a coupled reaction in which glutamate dehydrogenase uses the glutamate generated by glutaminase to produce NADH, which is detected by measuring absorbance at 340nm for 5 minutes. The data produced from this assay can be used to calculate the initial rate of the reaction (V_0), the maximal rate of the reaction (V_{max}), the Michaelis-Menten constant (K_m), the rate of turnover of enzyme (K_{cat}), and finally the enzyme efficiency (K_{cat}/K_m) as described in Section 2.2.4. Collectively, these measurements allowed me to compare the four enzymes: WT, R272K, S482C and L606R.

I measured glutaminase activity as production of NADH over time using five concentrations of glutamine: 2.5mM, 5mM, 10mM, 20mM and 40mM. Parts A, B, C of Figure 2.3 (below) are the results of the three independent experiments, each comprising three technical replicates.

A

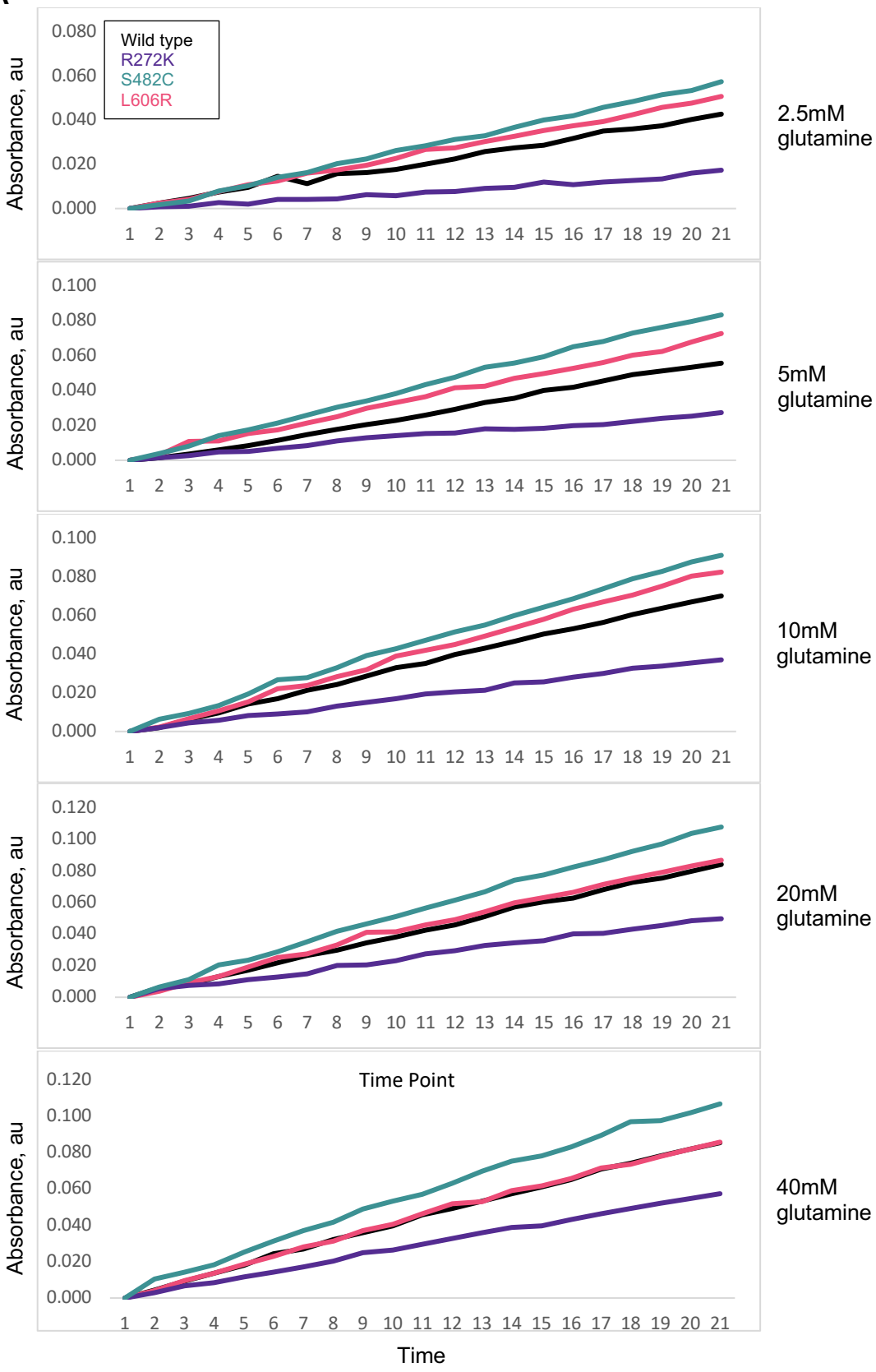
Wild type
R272K
S482C
L606R
Absorbance, au
Time Point
Time
2.5mM glutamine
5mM glutamine
10mM glutamine
20mM glutamine
40mM glutamine

B

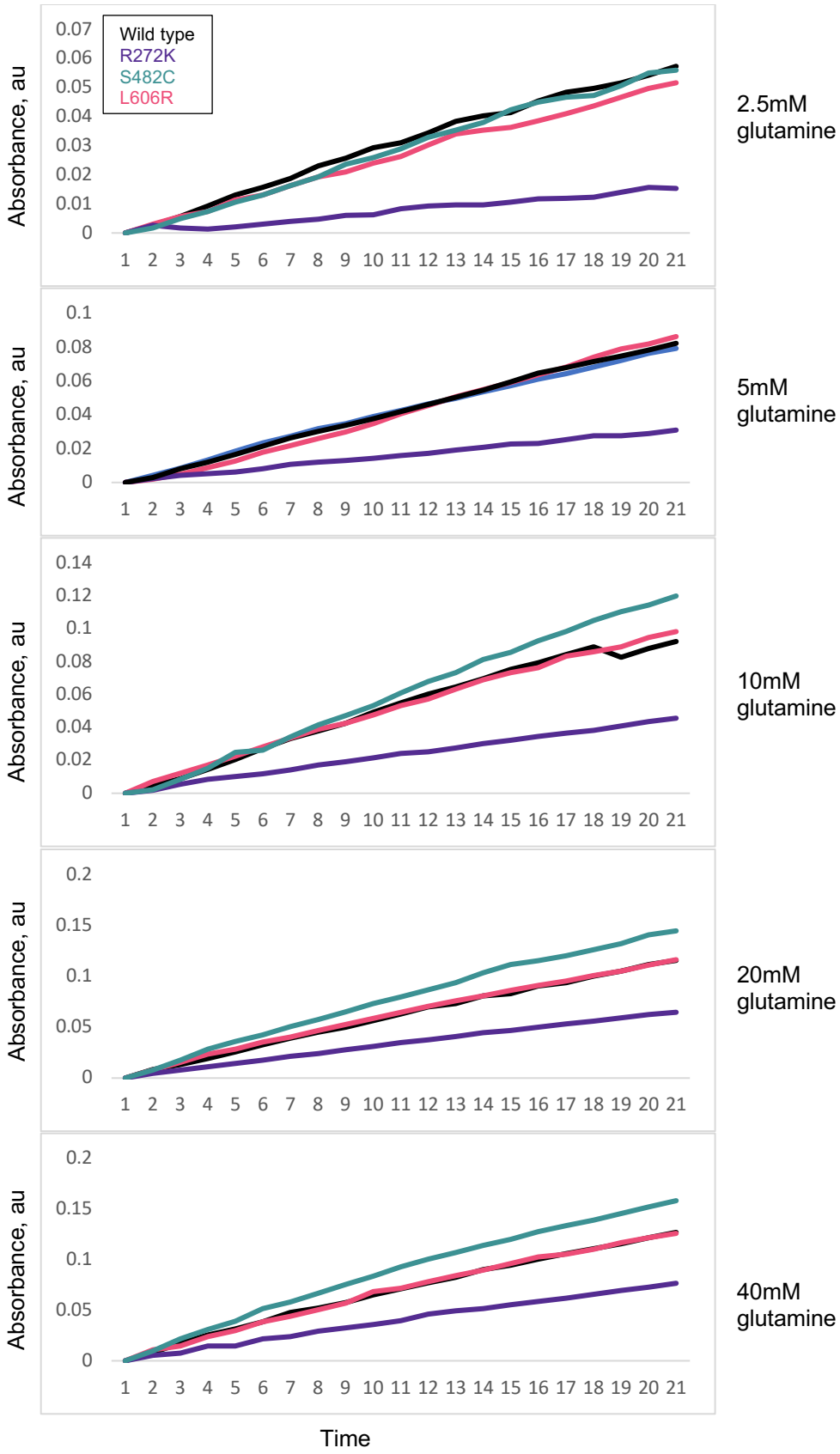
Wild type
R272K
S482C
L606R
Absorbance, au
Time
2.5mM glutamine
5mM glutamine
10mM glutamine
20mM glutamine
40mM glutamine

C

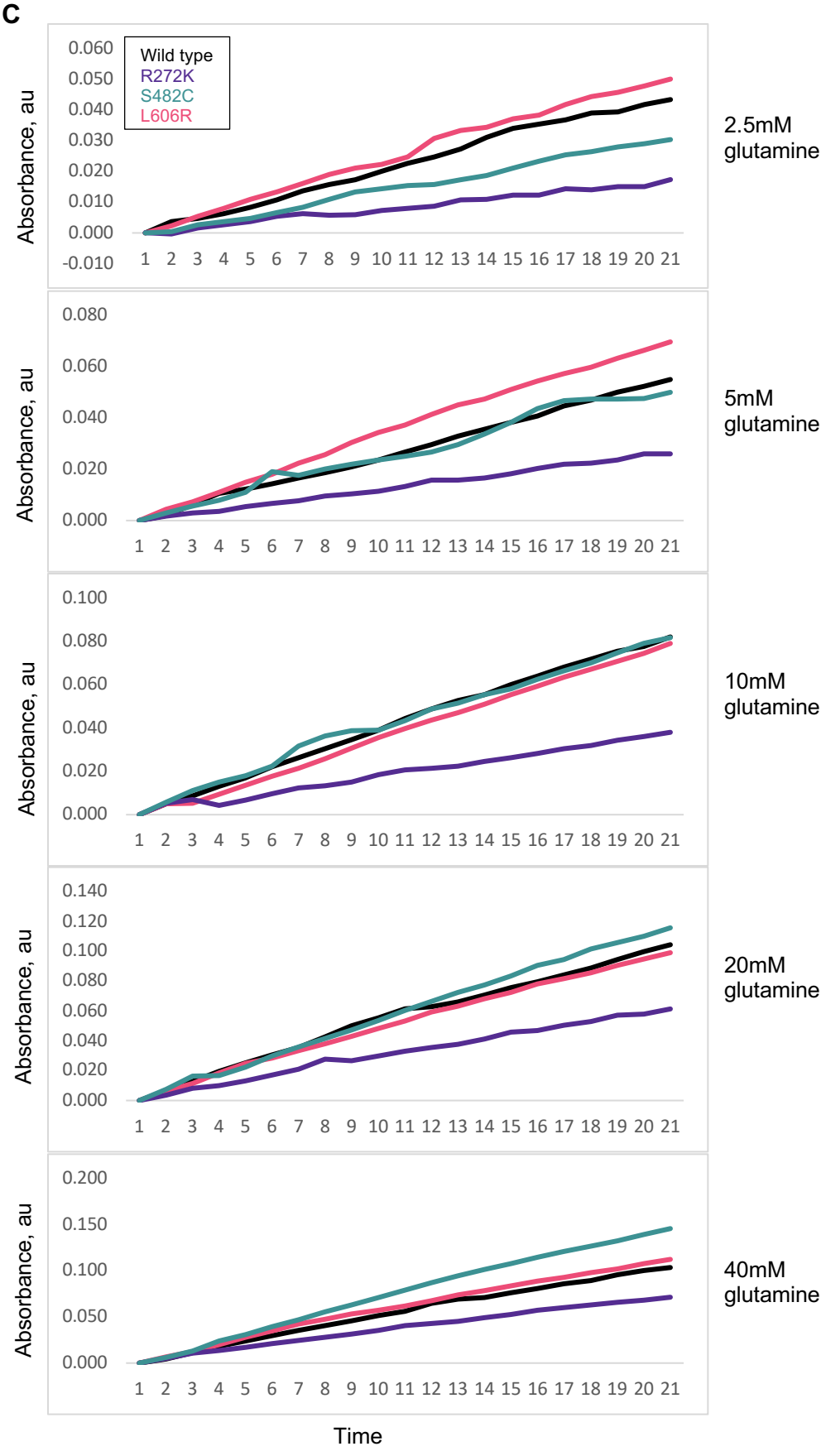
Wild type
R272K
S482C
L606R
Absorbance, au
0.060
0.050
0.040
0.030
0.020
0.010
0.000
-0.010
1 2 3 4 5 6 7 8 9 10 11 12 13 14 15 16 17 18 19 20 21
2.5mM glutamine
0.080
0.060
0.040
0.020
0.000
5mM glutamine
0.100
0.080
0.060
0.040
0.020
0.000
10mM glutamine
0.140
0.120
0.100
0.080
0.060
0.040
0.020
0.000
20mM glutamine
0.200
0.150
0.100
0.050
0.000
40mM glutamine
Time

Figure 2.3. **Production of NADH over time.**
Production of NADH was measured by absorbance at 340nm, with 10nM enzyme at each glutamine concentration. A, B, C are three independent experiments, each with three replicates

The mutant enzyme R272K (purple) produced less NADH than did wild-type enzyme (black) at all substrate concentrations. The mutant enzyme S482C (green) produced more NADH than did wild-type in experiment 1 (Figure 2.3A), but was more variable in experiments 2 and 3 (Figure 2.3B,C). The mutant enzyme L606R (pink) of our patient produced more NADH than did wild-type enzyme at lower glutamine concentrations but was very similar to wild-type at higher glutamine concentrations. This result suggests that the L606R enzyme is more sensitive to low substrate concentrations than is WT.

For each enzyme at each glutamine concentration I calculated the slope of the line indicating NADH production over time to obtain the initial rate of the reaction, or initial velocity, V_0 (Table 2.1). NADH in picomoles per second was calculated using an extinction coefficient for NADH of 6220 M^{-1} at 340nm and 0.5cm path length. Total reaction volume was 200 microliters.

Table 2.1 **Initial velocity (V_0) of WT, R272K, S482C and L606R enzymes, 10nM enzyme**

V_0, au.s^{-1} (x10^5)

Glutamine , mM	WT	R272K	S482C	L606R
2.5	16.00 ± 2.86	5.33 ± 0.17	16.43 ± 5.13	16.97 ± 0.22
5	21.34 ± 4.26	9.46 ± 0.98	24.44 ± 6.24	25.63 ± 3.93
10	27.94 ±4.31	13.71 ± 1.83	32.81 ± 7.94	29.23 ± 3.03
20	33.01 ±5.21	18.98 ± 3.56	40.89 ± 6.57	33.56 ± 4.43
40	35.02 ±6.47	27.27 ± 4.38	44.29 ± 8.59	34.32 ± 6.96

V_0, NADH picomol.s^{-1}

Glutamine , mM	WT	R272K	S482C	L606R
2.5	10.29 ± 1.84	3.42 ± 0.11	10.56 ± 3.30	10.91 ± 0.14
5	13.72 ± 2.74	6.08 ± 0.63	15.72 ± 4.01	16.48 ± 2.53
10	17.97 ± 2.77	8.81 ± 1.18	21.10 ± 5.10	18.80 ± 1.95
20	21.23 ± 3.35	12.21 ± 2.29	26.30 ± 4.23	21.58 ± 2.85
40	22.52 ± 4.16	14.32 ± 2.82	28.49 ± 5.52	22.07 ± 4.41

As expected, for each enzyme, V_0 increases with increased substrate concentration. As described in Section 2.2.4, I calculated the non-linear regression of V_0 in picomol.s^{-1} versus substrate concentration, using GraphPad Prism 8.1.2, to create Michaelis-Menten curves. These curves illustrate the rate of reaction at each concentration of glutamine. The S482C enzyme has higher V_0 values than WT enzyme ($P = 0.03$), particularly at higher substrate concentrations, while the R272K enzyme has lower V_0 values across the range of concentrations ($P < 0.0001$). V_0 values for the L606R enzyme were slightly higher than WT for lower concentrations of substrate but did not differ significantly overall ($P = 0.20$).

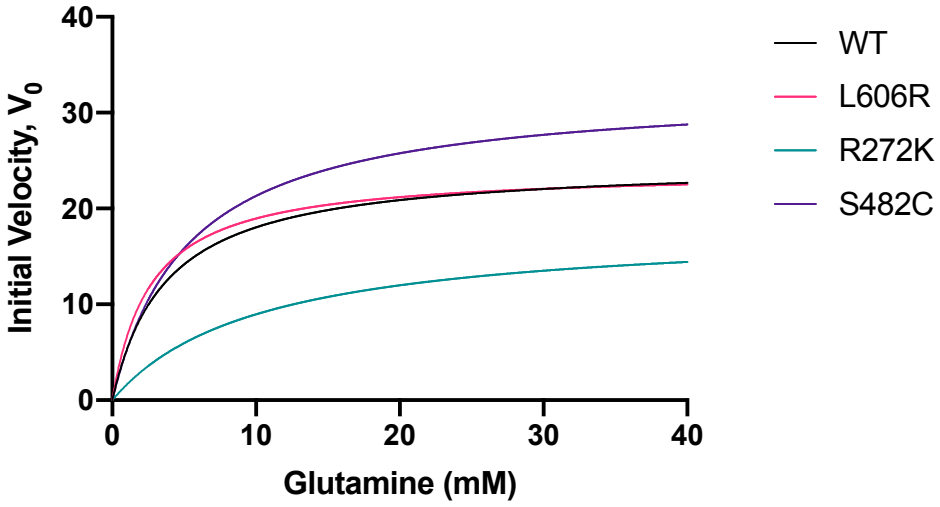

Figure 2.4. **Michaelis-Menten curves of the four enzymes from 2.5mM-40mM glutamine, 10 nM enzyme**

Next, I calculated the kinetic parameters for each enzyme, as described in Section 2.2.4 (Table 2.2). V_{max} values of the mutant enzymes did not differ significantly from WT. Average Michaelis-Menten constants (K_m) and average turnover values (K_{cat}) differed considerably across the four enzymes, but given the variability across experiments, no differences were significant. In contrast, the K_{cat}/K_m ratio was significantly lower for the R272K enzyme than for

WT (P = 0.009) and marginally higher for the L606R enzyme than for WT (P = 0.057), but no different for the S482C enzyme (P = 0.74) (Figure 2.5).

Enzymes S482C and L606R appear to be activating for different reasons. The S482C enzyme carries out its reactions significantly more rapidly, reflected in velocity (Figure 2.4). The L606R enzyme is activating by being more efficient in its affinity to substrate (Table 2.2).

Table 2.2. **Kinetic parameters of wild type and mutant glutaminase enzymes at 10nM.**

	V_{max} (picomol.s^{-1})	K_m (mM)	K_{cat} (s^{-1})	K_{cat}/K_m ($mM^{-1}.s^{-1}$)
Wild type	24.86 ± 4.38	3.79 ± 0.89	12.43 ± 2.19	3.35 ± 0.72
R272K	29.82 ± 20.45	25.18 ± 26.16	12.05 + 2.21	0.88 ± 0.58
S482C	33.92 ± 8.18	6.48 ± 5.10	16.96 ± 4.09	3.65 ± 2.01
L606R	24.10 ± 4.43	2.67 ± 0.73	12.05 ± 2.21	4.62 ± 0.65

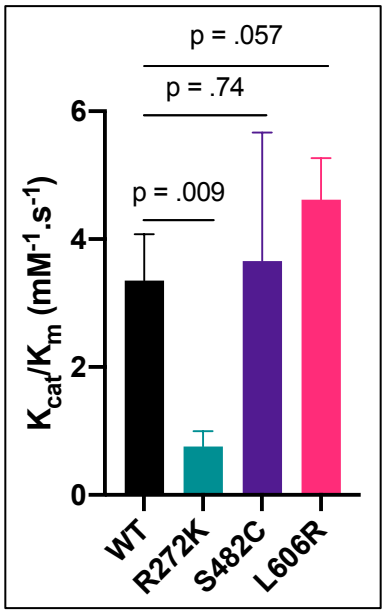

Figure 2.5. **Comparison of K_{cat}/K_m between wild type and mutant enzymes.**

The L606R enzyme of our patient has the highest affinity for glutamine and is the most efficient of the enzymes tested, supporting my hypothesis that the L606R mutation results in a hyperactive enzyme. Interestingly, although the V_{max} and K_{cat} values are similar between WT and L606R, the L606R mutation seems to cause an increase in affinity for glutamine which results in a more efficient enzyme. The other hyperactive allele, S482C, has a higher V_0 rate but is not more efficient than L606R because its affinity for glutamine is not as high.

As suggested above, I speculate that L606R is hyperactive because the mutation destabilizes binding of ankyrin repeats, promoting the production of long filaments with increased catalytic activity. It is possible to test the length of filament formation as described by Pasqualli et al.[21] Briefly, the purified protein generated for the enzymatic assays could be further purified with an ion exchange column followed by selection of the expected band size using size-exclusion chromatography. To activate the enzyme and induce the formation of higher order species, inorganic phosphate can be added to the ultra-pure protein and the particle size can be analyzed using gel filtration chromatography.

2.3.2 Analysis of metabolites in lymphoblast cells

Rumping et al. identified differences in the glutamate to glutamine ratio in a patient with the activating glutaminase mutation S482C.[41] Because glutamate, glutamine and the products of their reactions are involved in multiple metabolic pathways, I wondered whether there might be differences in metabolites beyond the two directly involved in the glutaminase reaction. Technical advances in analytical chemistry now enable the simultaneous detection of multiple metabolites from biological samples.[50] I sought to analyze the metabolic profile of lymphoblast cell lines from the patient and his unaffected parents.

Targeted aqueous metabolite profiling analysis was performed at the Northwest Metabolomics Research Center on a total of eight replicate cell pellets from each individual using hydrophilic interaction chromatography (HILIC) MS/MS. A total of 155 metabolites were

detected, 75 in the positive ion mode and 80 in the negative ion mode. The analytes were normalized to log-transformed total ion current, and t-tests of each metabolite comparing the patient to his unaffected parents were performed. After correcting for multiple comparisons, there were a total of eight metabolites that were significantly different between the cells of the patient and his parents (Table 2.3).

Table 2.3. **Metabolites with significantly different levels in lymphoblast cells of patient and his unaffected parents**

Metabolite	Ion Mode	Description	P-value	Effect in patient
N-Acetyl-aspartyl-glutamate (NAAG)	Negative	Neuropeptide, acetylated amino acid	1.81E-09	↑
Inosine monophosphate (IMP)	Negative	Purine metabolism	6.39E-06	↑
NAAG + glutamic acid (total glutamate)	Both	Amino acid	3.83E-06	↑
Glutamine	Positive	Amino acid	9.47E-05	↑
Lactate	Negative	Glycolysis/TCA pathway	2.62E-04	↑
Pentothenate	Negative	Vitamin B5 anion	3.31E-04	↓
Uracil	Negative	Nucleotide/Pyrimidine metabolism	5.18E-04	↓
Methionine sulfoxide	Positive	Methionine oxidative stress product	6.37E-04	↑
Thiamine	Positive	Vitamin B1	8.77E-04	↓

Intriguingly, the metabolite most significantly different in level of expression between cells of the proband and his parents is N-acetyl-aspartate-glutamate (NAAG), a peptide neurotransmitter that has multiple functions in the central nervous system and is concentrated at synaptic vesicles and neurons.[51] NAAG is formed by the addition of glutamate to N-acetyl-L-aspartate by the enzyme N-acetyl-aspartyl-glutamate synthetase B (encoded by the *RIMKLB* gene). Both glutamate (P = 0.01) and glutamine (P = 0.00009) were also significantly increased in the cells of the patient compared to his parents.

In fibroblasts of the patient with the activating S482C mutation, the glutamate / glutamine ratio was higher than in fibroblasts of controls. Similarly, in lymphoblasts of our patient with the

L606R mutation, the glutamate / glutamine ratio was higher than in the cells of his unaffected parents. Total glutamate was measured as the sum of NAAG and glutamic acid as combined contribution to the total metabolic profile. The glutamate / glutamine ratio for the proband is 1.97 ± 0.05, for the unaffected mother 1.90 ± 0.04, and for the unaffected father 1.88 ± 0.06 (P = 0.002 for proband vs both parents).

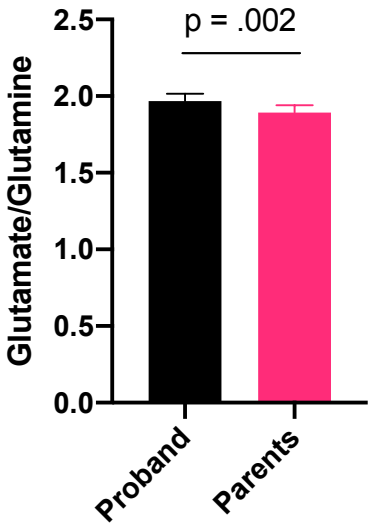

Figure 2.6. **Glutamate/glutamine ratio in lymphoblast cell lines from patient and his parents.**

Of the eight metabolites with significantly different cellular levels in the proband compared to his parents, two metabolites are involved in nucleotide synthesis. Inosine monophosphate (IMP), which is elevated in the patient compared to his parents, is the first nucleoside formed during purine synthesis and accepts nitrogen from glutamine. In contrast, uracil, which is found at lower levels in the patient, is a pyrimidine derivative whose synthesis involves glutamine donation of nitrogen and carbon dioxide.

B-vitamin levels were also significantly different in cells from the patient compared to his parents. Both thiamine (vitamin B1) and pantothenate (the anion of vitamin B5) were reduced in the patient. Thiamine is a coenzyme that is important to the citric acid cycle and pentose phosphate pathway. Pantothenate is a component of coenzyme A, which is important for carbon

transport within the cell. Deficiencies in B vitamins can cause fatigue, irritability, confusion and encephalopathy.[52]

Methionine sulfoxide, a marker of oxidative stress and cellular aging, was increased in the patient. Because excess glutamate leads to an increase in oxidative stress, Rumping et al investigated how the S482C activating mutation affected scavenging of reactive oxygen species.[41] They found that cells overexpressing the mutant protein had an increase in reactive oxygen species, indicating that hyperactive glutaminase which generates excess glutamate can lead to oxidative stress. Other metabolites from the oxidative damage pathway in our panel (malondialdehyde and reduced or oxidized glutathione) did not differ between the patient and his parents.

The final metabolite that was significantly different in lymphoblast cell lines from the patient compared to his parents is lactate, which is increased in the patient. Lactate is formed during anaerobic conditions from pyruvate by pyruvate dehydrogenase. Lactate participates in the Cori cycle, in which lactate formed via anaerobic glycolysis in muscles is transferred to the liver where it is converted to glucose. Increased lactate can also be due to many causes including acute illness, drugs or toxins, mitochondrial disease, and thiamine deficiency. The increased lactate of the patient may be a consequence of his lower levels of thiamine.

Performing a targeted metabolic profile of lymphoblast cell lines from the patient and his parents provided a more in-depth examination of the potential consequences of altered glutaminase activity. Both NAAG, which is a neurotransmitter that contains glutamate, glutamate and glutamine were significantly elevated in the patient. Other metabolic alterations included nucleotide synthesis, B vitamins, oxidative stress and lactate.

2.3.3 Characterization of iPSCs

Glutaminase plays a key role in the proper maintenance, self-renewal and differentiation of neural stem cells.[24] In order to determine whether these processes were affected in the patient cells, I set out to establish pluripotent stem cell lines of the patient and his parents that I could differentiate into a mixed neuronal culture. Lymphoblast cell lines from the proband and his father were reprogrammed into induced pluripotent stem cells (iPSCs). Reprogramming of the mother's cell line was attempted but was unsuccessful. The proband and father's iPSC cell lines were characterized by morphology, pluripotency and karyotype (Figure 2.7).

The gross morphology of iPSC colonies was compared to H9 human embryonic stem cells that were maintained under identical conditions.[53] Pluripotent stem cells form colonies of tightly packed cells that aggregate into a rounded shape with smooth edges. Both the proband and father's iPSCs had pluripotent stem cell colony morphology. Colonies of both the proband and father were positive for the pluripotency marker OCT4 and both had normal karyotypes by Giemsa banding analysis. These data establish that the lymphoblast cell lines from both the proband and the father were successfully reprogrammed to iPSCs.

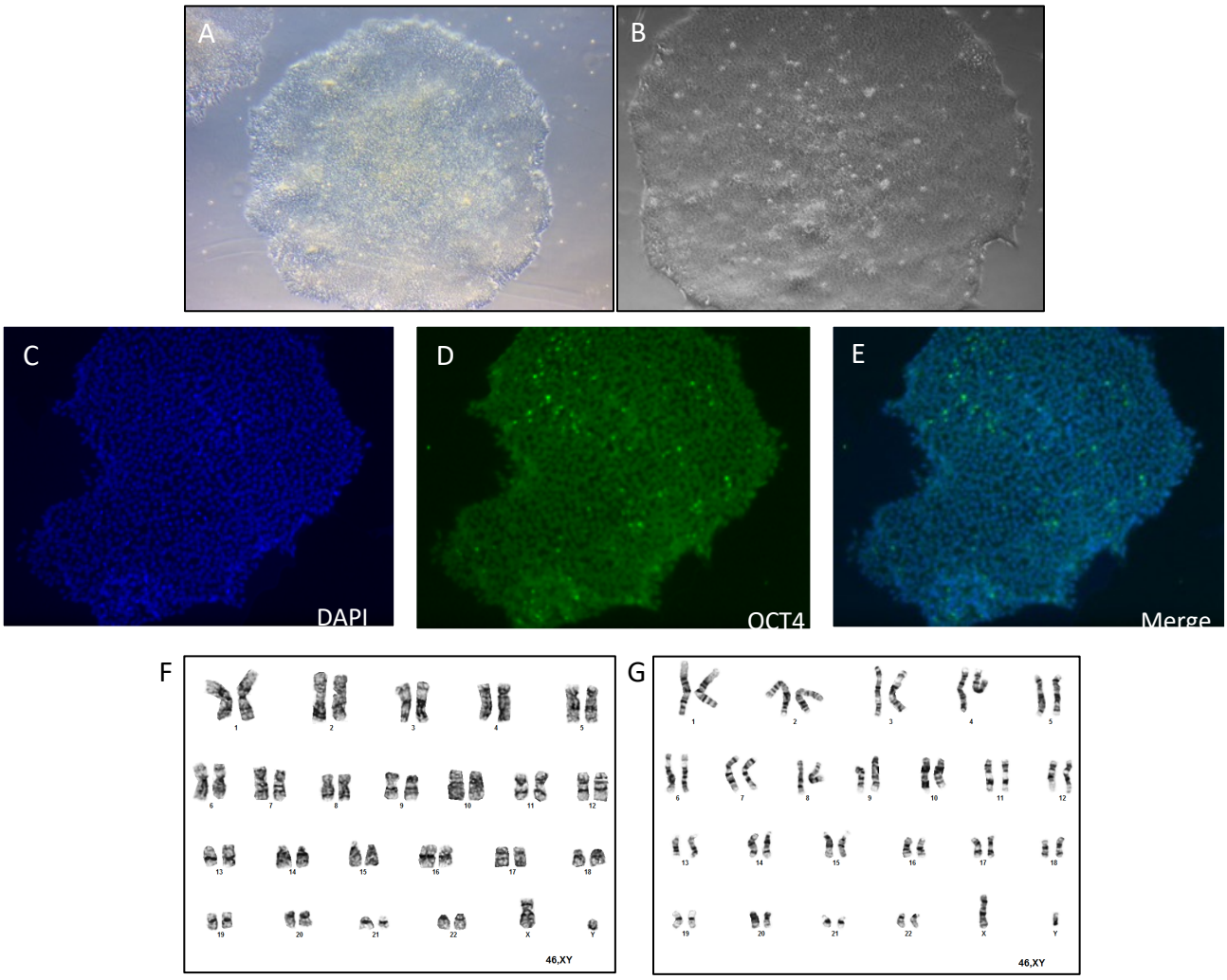

***Figure 2.7*. iPSCs derived from lymphoblast cell lines of the proband and father**
(A,B) Gross morphology of embryonic stem cell (A) and iPSC (B). Both colonies are tightly packed and round with smoothed edges. There is no evidence of contaminating cell types. (C,D,E) Immunofluorescence analysis of iPSCs with DAPI (C) and OCT4 (D) shows that the entire colony is pluripotent (E). (F,G) Giemsa banding confirmed that iPSC cell lines from the proband (F) and father (G) iPSC lines had normal karyotypes.

2.3.4 Glutamate and glutamine in iPSCs

Metabolic profiling of differentiating mouse primary cortical neurons has revealed that there is a significant increase in glutamate (but not glutamine) levels as differentiation

proceeds.[54] In fibroblast cells from the patient with the hyperactive S482C enzyme, there was an increased glutamate/glutamine ratio.[41]

These lines of evidence led me to hypothesize that there might be an increase in the glutamate/glutamine ratio in a mixed neuronal culture differentiated from iPSCs of the proband compared to his father. Attempts at differentiating the iPSCs into neurons were unsuccessful. For successful differentiation of iPSCs, it is imperative that the colonies are of high quality and have very little spontaneous differentiation (<10%). Although the iPSCs from the patient and his father were confirmed pluripotent and had normal karyotypes, they exhibited high levels of spontaneous differentiation after thawing fresh aliquots. The initial reprogramming and morphological descriptions from Section 2.3.3 were performed in a different tissue culture room, and potentially slightly different incubator conditions (e.g. % CO_2). Some spontaneous differentiation was identified in the original iPSC colonies after passage 18, however after thawing fresh aliquots in the new tissue culture room spontaneous differentiation arose after just 4 passages. Despite the spontaneous differentiation, I attempted the neuronal differentiation protocol after manually removing the colonies exhibiting differentiation. It is possible that the low quality of the starting iPSCs (i.e. their tendency towards spontaneous differentiation) was what caused the unsuccessful differentiation. Meanwhile, another group also reported that they were unsuccessful differentiating iPSCs from patients with glutaminase deficiency into neurons, although they did not specify at which point during differentiation their cells failed.[40] To determine whether the unsuccessful differentiations were due to the genotype it would be important to generate the patient mutations using gene editing such as CRISPR/Cas9 in an isogenic human embryonic stem cell line or a control iPSC line.

Due to the difficulties encountered during differentiation, I sought to determine whether intracellular glutamate levels were altered in the pluripotent state. Using a luminescence-based assay, I determined that intracellular glutamate and the glutamate/glutamine ratio were both slightly higher in iPSCs from the father compared to the proband (Figure 2.8).

This result is the opposite of that from the metabolite analysis (Section 2.3.3). There are several possible reasons why the observed glutamate/glutamine ratio was slightly higher in the father compared to the proband. Due to the limited number of cells available, the assay results were from a single experiment with four replicates. Although every attempt was made, the iPSC lines were not at the same point of the growth curve so it is possible that differences in growth and therefore metabolic rate may be reflected in these levels. Because a full metabolite analysis was not performed on these cells due to limited material, it is also possible that there are downstream metabolites that would reflect a difference, including NAAG. Finally, because the proband did not develop symptoms until 16 years of age, the pathogenic effects of the glutaminase mutation may not become evident until later in development so they may not be reflected in cells from early in development.

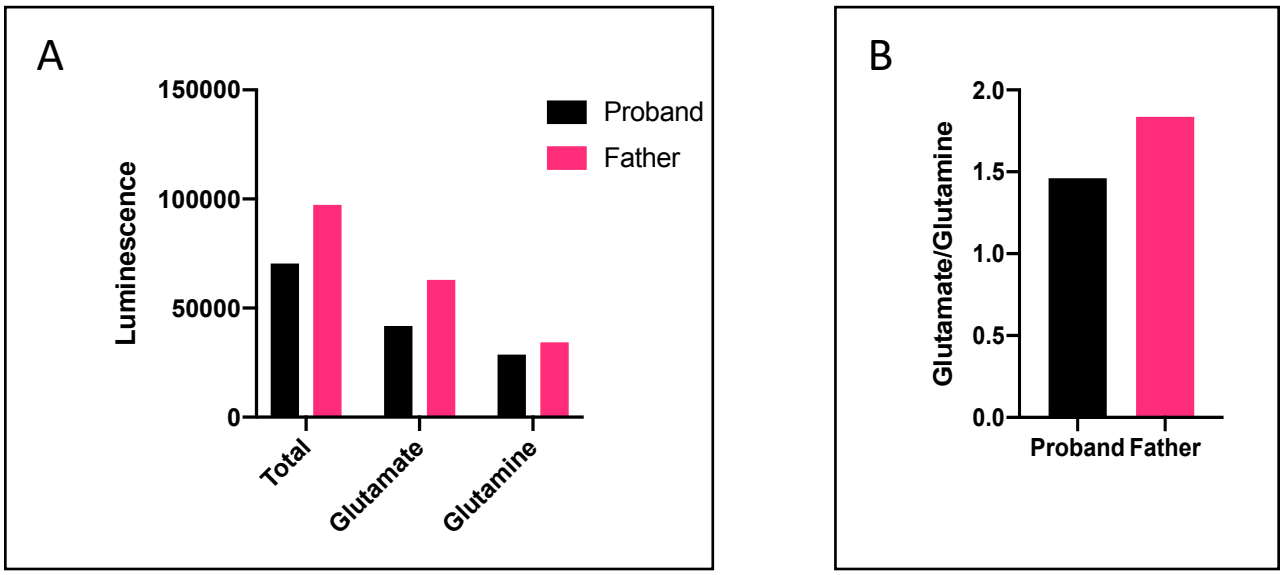

***Figure 2.8*. Glutamate and glutamine in iPSCs.**
(A) Glutamate and glutamine. (B) Glutamate/glutamine ratio

Chapter 3: Conclusions

3.1 Summary

The goal of this dissertation project was to functionally characterize a *de novo* mutation in glutaminase that was identified in an individual with bipolar disorder with psychosis. I began the project with the hypothesis that the L606R mutation caused a hyperactive enzyme, and that this gain of function could lead to alterations in the metabolic profile from biological tissue of the patient. Observations from enzyme assays and a targeted metabolite analysis support my hypothesis that the L606R mutation causes an increase in enzymatic activity and alterations to the metabolite profile of the patient.

Reports of human disease-causing mutations in glutaminase have just begun to be published making glutaminase an emerging disease gene. This is the first description of a mutation in glutaminase in an individual with a psychiatric disorder.

3.2 Discussion

The kinetic data indicate that the L606R mutation in *GLS* results in a more efficient enzyme than WT, and in an elevated glutamate/glutamine ratio. The other activating mutation, S428C, yields a more active enzyme and similarly an elevated glutamate / glutamine ratio.[41] Our patient is less severely affected that the patient carrying the S482C mutation. Both mutations are *de novo* and heterozygous in the patients, but S482C lies in the glutaminase catalytic domain whereas L606R is located within the ankyrin repeat domain, potentially altering tertiary protein structure.

The patient's lymphoblasts and iPSCs both showed an increased level of glutamine compared to his parents (or his father for the iPSC analysis). Glutamine levels in extracellular fluid in the brain and cerebral spinal fluid are generally significantly higher than any other amino acid, including glutamate, however in some regions of rat and rabbit brain, glutamine levels are

slightly lower than glutamate.[55] In models of hepatic encephalopathy where an excess of glutamine is associated with hyperammonemia, there is evidence of mitochondrial damage and edema related to enlarged astrocytes.[55] Glutamine participates in many metabolic pathways and is readily transported across the blood-brain-barrier. Therefore, it is possible that the excess glutamine is not directly causing a psychiatric phenotype in this patient.

In addition to excess glutamine, total glutamate levels are significantly higher in the patient. An excess of glutamate can lead to the overexcitation of neurons and has been shown to cause cellular damage or death at high enough levels. Our patient responded successfully to lithium treatment. Chronic lithium treatment reduced glutamate uptake in synaptosomes from mice[20], and protected against excitotoxicity in a rat neuronal culture by inhibiting calcium influx mediated by N-methyl-D-aspartate (NMDA) receptors.[56] These lines of evidence provide a mechanism by which lithium can help to normalize glutamate levels at the synapse, reducing potential over-excitation.

The patient also has significantly increased levels of N-acetyl-aspartyl-glutamate (NAAG), which consists of glutamate and N-acetyl-aspartate. This peptide neurotransmitter is formed by N-acetyl-aspartyl-glutamate synthetase B (encoded by the *RIMKLB* gene) and is cleaved by glutamate carboxypeptidase II (GCPII; encoded by the *FOLH1* gene). NAAG has been shown to be an agonist of metabotropic glutamate receptors, leading to inhibition of the release of neurotransmitters, including glutamate.[57] In a phencyclidine (PCP) model of schizophrenia, Zuo et al showed that inhibition of GCPII resulted in decreased glutamate release in the medial prefrontal cortex and nucleus accumbens in rat.[58] The increased levels of NAAG in our patient may help to downregulate the excess glutamate produced by the patient's hyperactive glutaminase.

Figure 3.1 is a model for the action of GLS p.L606R. The mutation leads to increased enzymatic efficiency compared to wild type. The excess of glutamate in patient cells may result in overexcitation of neurons which can be inhibited by both lithium treatment and an excess of

NAAG. Collectively, these results directly link a rare damaging *de novo* mutation in an enzyme to the biological mechanism of successful treatment of a patient with bipolar disorder with psychosis using lithium.

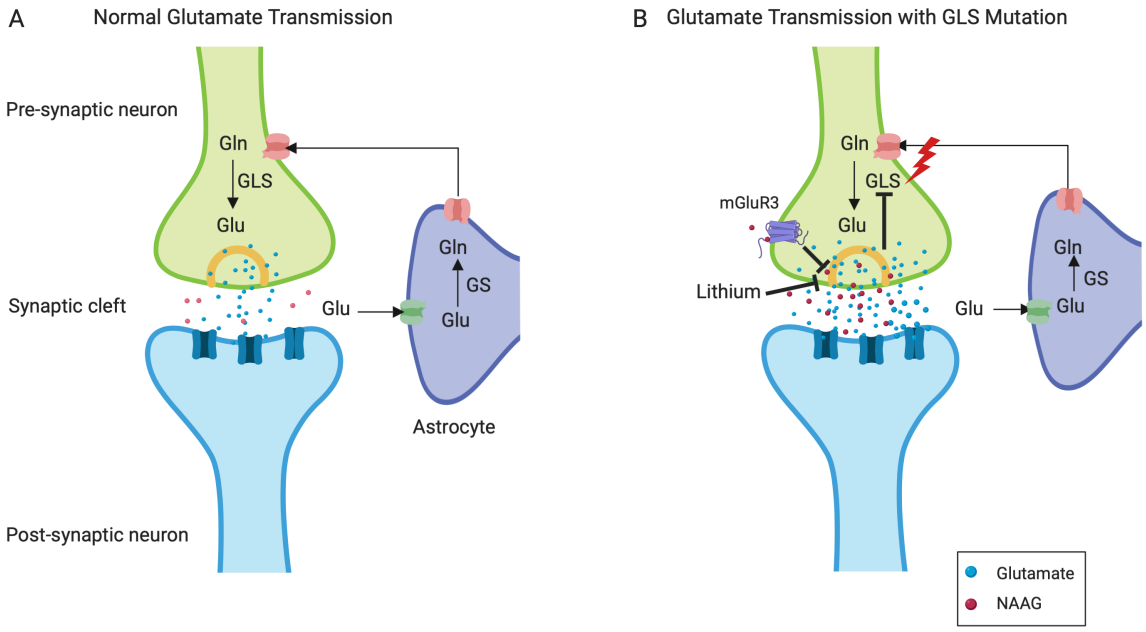

***Figure 3.1* Model of altered glutamate recycling in patient with GLS p.L606R.**
A. Normal glutamate transmission. Glutamate from the synaptic cleft is taken up by astrocytes, where it is converted to glutamine by glutamine synthetase (GS). Glutamine is then transported back to pre-synaptic neurons where glutaminase (GLS) converts it back to glutamate.
B. GLS p.L606R results in increased levels of glutamate at the synaptic cleft. This excess glutamate is controlled by lithium, which inhibits uptake of glutamate into synapses, and by NAAG, which inhibits release of glutamate through the glutamate receptor (mGluR3).

Inborn errors of metabolism typically present with deficiency of an enzyme, however both loss of function and gain of function mutations have been identified in *GLS*. The genetic lesions in *GLS* include point mutations, frameshifts, and repeat expansions. Along with the range of genetic mechanisms discovered in patients with mutations in *GLS*, there is also a wide range of phenotypes and age of onset. Loss of function mutations have been associated with ataxia, developmental delay and epileptic encephalopathy and age of onset ranged from

neonatal to 7 years. The gain of function mutations result in profound developmental delay, cataract and bipolar disorder with psychosis and age of onset is infancy to 16 years old. Mice with overexpression of the GAC isoform showed learning deficits and synaptic dysfunction.[59] Mice with complete loss of glutaminase function die of respiratory insufficiency on postnatal day 1.[46] The human allele with the most severe loss of function also leads to neonatal mortality involving respiratory insufficiency.[39] The other reported human alleles likely retain some function, with several patients surviving past age 20 years.

Differences in severity and age of onset of *GLS*-associated conditions may be due to dosage effects of the specific *GLS* mutations. When glutaminase activity is significantly lower or higher than normal, phenotypes are more severe and present earlier in life. If loss- or gain- of function is not complete, the phenotype may present later.

For conditions with later age of onset, it is still unknown what mechanisms may trigger symptoms. Because our patient developed symptoms when he was 16 years old, I wondered if hormonal changes during puberty might affect glutamate levels changing the level of activity required of the mutant glutaminase. Interestingly, studies in rats have revealed that there is an increase in glutamate release as well as an increase in glutaminase expression in the hypothalamus during puberty.[60] Glutamate release has also been shown to increase during puberty in non-human primates when luteinizing hormone levels increase.[61] It is possible that the requirement for increased glutamate during puberty could exacerbate the effects of the mutation in our patient, thereby contributing to his onset of symptoms.

3.3 Future Directions

A limitation to the glutaminase enzymatic activity assay is the high variability in replicate experiments. There is an increase in variability the longer the purified proteins are stored, leading me to believe that there is potentially some degradation of the proteins or they are somehow interacting with other species present in the preparation. There are several ways to

determine what is causing the variability, including further purifying the proteins using ion exchange chromatography and size-exclusion chromatography or to prepare a fresh batch of purified protein to see if variability again increases over time.

One limitation of this study was the cell type used for metabolite analysis. Both lymphoblast cell lines and fibroblasts derived directly from the patient are commonly used to test hypotheses generated from genetic studies. However, these cell lines may not accurately reflect the molecular and metabolic pathways that are active in the cells and tissues affected in the patient. This is especially the case for neurological and psychiatric disorders where it is not possible to sample brain tissue. Because of this limitation, pluripotent stem cell models have become important tools for studying neurological phenotypes. These models allow us to differentiate cells into appropriate cell types that have the genetic background that best helps test hypotheses. Stem cell technology has advanced rapidly, and now allows us to model complex tissues with multiple cell types such as the human brain in 3D. Using both 2D and 3D stem cell models can help us understand how genetic variants might alter neurotransmission, morphological changes, calcium signaling and changes in gene expression in neurons. Interestingly, pluripotent stem cells derived from patients with *GLS1* mutations fail to properly differentiate into neurons. This may be due to the importance of glutaminase in proliferation, maintenance, and differentiation of neural stem cells. It would be important to follow up on the reasons for failed differentiation, since our patient lived to adulthood, as did the other patients with partial loss of function mutations whose iPSCs failed differentiation.[40] Introducing the specific mutations in an isogenic cell line and attempting differentiation may provide further information on the impact of the actual mutation without the genetic background from the patients. Performing cell growth curves, metabolite analysis, viability tests and RNA-seq may help elucidate potential mechanisms for failed or altered differentiation in cells carrying the mutation.

An additional limitation of the metabolite study was that a single patient with a *GLS* mutation was compared to his parents. Expanding this investigation to include cell lines from additional patients with mutations in *GLS* as well as additional controls would determine the normal range of metabolite levels and further identify metabolites that are consistently affected when there is an alteration in *GLS*.

Genetic studies provide insight into the potential molecular pathogenicity of disease. The recent discoveries of human disease-causing mutations in glutaminase in patients with diverse neurological phenotypes establishes *GLS* as a gene for neurological illnesses. To my knowledge, this is the first description of the biochemical and metabolic consequences of a *GLS* mutation in a psychiatric disorder.

Studies attempting to identify common alleles for psychiatric disorders have so far not robustly identified candidate genetic loci. The most likely reason for this is the underlying genetic heterogeneity of psychiatric disorders. Genetic causes of psychiatric disorders are more likely to be rare with larger effect size. Indeed, studies looking for rare damaging mutations have begun to provide promising results. Rare mutations in coding and non-coding portions of both inhibitory and excitatory neurotransmission have been discovered in individuals with BD. The psychiatric genetics field will likely gain momentum as more studies investigate the role of rare variants. Targeted re-sequencing of genes and pathways currently implicated in psychiatric disorders can further refine our understanding of the molecular mechanisms of these complex disorders. Because *GLS1* has recently emerged as a human disease-causing gene, it will be interesting to specifically sequence this gene and its non-coding regions in individuals with developmental delay and psychiatric disorders.

References

1 Dunayevich E and Keck PE. Prevalence and description of psychotic features in bipolar mania. Curr Psychiatry Rep. 2(4):286-290, 2000.

2 Schwartz JE, Fennig S, Tanenberg-Karant M, Carlson G, Craig T, Galambos N, Lavelle J, Bromet EJ. Congruence of diagnoses 2 years after a first-admission diagnosis of psychosis. Arch Gen Psychiatry. 57(6):593-600, 2000.

3 McGuffin P, Rijsdijk F, Andrew M, Sham P, Katz R, Cardno A. The heritability of bipolar affective disorder and the genetic relationship to unipolar depression. Arch Gen Psychiatry. 60(5):497-502, 2003.

4 Craddock N and Jones I. Genetics of bipolar disorder. J Med Genet. 36:585-594, 1999.

5 Craddock N and Sklar P. Genetics of bipolar disorder. Lancet. 381:1654-1666, 2013.

6 Malhotra D and Sebat J. CNVs: Harbinger of a rare variant revolution in psychiatric genetics. Cell. 148(6):1223-1241, 2012.

7 Grozeva D, Kirov G, Ivanov D, Jones IR, Jones L, Green EK, St Clair DM, Young AH, Ferrier N, Farmer AE, et al. Rare copy number variants: A point of rarity in genetic risk for bipolar disorder and schizophrenia. Arch Gen Psychiatry. 67(4):318-327, 2010.

8 McQuillin A, Bass N, Anjorin A, Lawrence J, Kandaswamy R, Lydall G, Moran J, Sklar P, Purcell S, Gurling H. Analysis of genetic deletions and duplications in the University College London bipolar disorder case-control sample. Eur J Hum Genet. 19(5):588-592, 2011.

9 Noor A, Lionel AC, Cohen-Woods S, Moghimi N, Rucker J, Fennell A, Thiruvahindrapuram B, Kaufman L, Degagne B, Wei J, et al. Copy number variant study of bipolar disorder in Canadian and UK populations implicates synaptic genes. Am J Med Genet B Neuropsychiatr Genet. 165B(4):303-313, 2014.

10 Charney AW, Stahl EA, Green EK, Chen CY, Moran JL, Chambert K, Belliveau RA Jr, Forty L, Gordon-Smith K, Lee PH, et al. Contribution of rare copy number variants to bipolar disorder risk is limited to schizoaffective cases. Biol Psychiatry. 86(2):110-119, 2019.

11 Georgieva L, Rees E, Moran JL, Chambert KD, Milanova V, Craddock N, Purcell S, Sklar P, McCarroll S, Homans P, et al. De novo CNVs in bipolar affective disorder and schizophrenia. Hum Mol Genet. 23(24):6677-6683, 2014.

12 Green EK, Rees E, Walters JT, Smith KG, Forty L, Grozeva D, Moran JL, Sklar P, Ripke S, Chambert KD, et al. Copy number variation in bipolar disorder. Mol Psychiatry. 21(1):89-93, 2016.

13 Malhotra D, McCarthy S, Michaelson JJ, Vacic V, Burdick KE, Yoon S, Cichon S, Corvin A, Gary S, Gershon ES. High frequencies of de novo CNVs in bipolar disorder and schizophrenia. Neuron. 72:951-963, 2011.

14 Zhang D, Cheng L, Qian Y, Alliey-Rodriguez N, Kelsoe JR, Greenwood T, Nievergelt C, Barrett TB, McKinney R, Schork N, et al. Singleton deletions throughout the genome increase risk of bipolar disorder. Mol Psychiatry. 14(4):376-380, 2009.

15 Priebe L, Degenhardt FA, Herms S, Haenish B, Mattheisen M, Nieratschker V, Weingarten M, Witt S, Breuer R, Paul, T, et al. Genome-wide survey implicates the influence of copy number variants (CNVs) in the development of early-onset bipolar disorder. Mol Psychiatry. 17(4):421-432, 2012.

16 Ament SA, Szelinger S, Glusman G, Ashworth J, Hou L, Akula N, Shekhtman T, Badner JA, Brunkow ME, Mauldin DE, et al. Rare variants in neuronal excitability genes influence risk for bipolar disorder. Proc Natl Acad Sci USA. 112(11):3576-3581, 2015.

17 Kataoka M, Matoba N, Sawada T, Kazuno A-A, Ishiwata M, Fujii K, Matsuo K, Takata A, Kato T. Exome sequencing for bipolar disorder points to roles of de novo loss-of-function and protein-altering mutations. Mol Psychiatry. 21(7):885-893, 2016.

18 Eastwood SL and Harrison PJ. Markers of glutamate synaptic transmission and plasticity are increased in the anterior cingulate cortex in bipolar disorder. Biol Psychiatry. 67(11):1010-1016, 2010.

19 Hashimoto K, Sawa A and Iyo M. Increased levels of glutamate in brains from patients with mood disorders. Biol Psychiatry. 62(11):1310-1316, 2007.

20 Dixon JF and Hokin LE. Lithium acutely inhibits and chronically up-regulates and stabilizes glutamate uptake by presynaptic nerve endings in mouse cerebral cortex. Proc Natl Acad Sci USA. 95(14), 1998.

21 Pasqualli CC, Islam Z, Adamoski D, Ferreira IM, Righeto RD, Bettini J, Portugal RV, Yue WW, Gonzalez A, Dias SMG, Ambrosia ALB. The origin and evolution of human glutaminases and their atypical C-terminal ankyrin repeats. J Biol Chem. 292(27):11572-11585, 2017.

22 Ferreira APS, Cassago A, Goncalves KdA, Dias MM, Adamoski D, Axcencao CFR, Honorato RV, de Oliveira JF, Ferreira IM, Fornezari C, et al. Active glutaminase C self-assembles into a supratetrameric oligomer that can be disrupted by an allosteric inhibitor. J Biol Chem. 288(39):28009-28020, 2013.

23 Olalla L, Gutierrez A, Campos JA, Khan ZU, Alonso FJ, Segura JA, Marquez J, Aledo JC. Nuclear localization of L-type glutaminase in mammalian brain. J Biol Chem. 277(41):38939-38944, 2002.

24 Wang Y, Huang Y, Zhao L, Li Y, Zheng J. Glutaminase 1 is essential for the differentiation, proliferation, and survival of human neural progenitor cells. Stem Cells Dev. 23(22):2782-2790, 2014.

25 Zhao L, Huang Y and Zheng J. STAT1 regulates human glutaminase 1 promoter activity through multiple binding sites in HIV-1 infected macrophages. PLOS ONE. 8(9):e76581, 2013.

26 Wise DR, DeBerardinis RJ, Mancuso A, Sayed N, Zhang XY, Pfeiffer HK, Nissim I, Daikhin E, Yudkoff M, McMahon SB, Thompson CB. Myc regulates a transcriptional program that stimulates mitochondrial glutaminolysis and leads to glutamine addiction. Proc Natl Acad Sci USA. 105(48):18782-18787, 2008.

27 Rathore MG, Saumet A, Rossi JF, de Bettignies C, Tempe D, Lecellier CH, Villalba M. The NF-κB member p65 controls glutamine metabolism through miR-23a. Int J Biochem Cell Biol. 44(9):1448-1456, 2012.

28 Li J, Song P, Jiang T, Morrison H, Wang X, Jin H. Heat shock factor 1 epigenetically stimulates glutaminase-1-dependent mTOR activation to promote colorectal carcinogenesis. Mol Ther. 26(7):1828-1839, 2018.

29 Mellios N and Sur M. The emerging role of microRNAs in schizophrenia and autism spectrum disorders. Front Pyschiatry. 3(39):eCollection, 2012.

30 Kvamme E, Torgner IA, Roberg B. Kinetics and localization of brain phosphate activated glutaminase. J Neurosci Res. 66:951-958, 2001.

31 Cassago A, Ferreira APS, Ferreira IM, Fornezari C, Gomes ERM, Greene KS, Pereira HM, Garratt RC, Dias SMG, Ambrosio ALB. Mitochondrial localization and structure-based phosphate activation

mechanism of glutaminase C with implications for cancer metabolism. Proc Natl Acad Sci USA. 109(4):1092-1097, 2012.

32 Burbaeva G, Boksha IS, Tereshkina EB, Savushkina OK, Prokhorova TA, Vorobyeva EA. Glutamate and GABA-metabolizing enzymes in post-mortem cerebellum in Alzheimer's disease: Phosphate-activated glutaminase and glutamic acid decarboxylase. Cerebellum. 13(5):607-615, 2014.

33 D'Alessandro G, Calcagno E, Tartari S, Rizzardini M, Invemizzi RW, Cantoni L. Glutamate and glutathione interplay in a motor neuronal model of amyotrophic lateral sclerosis reveals altered energy metabolism. Neurobiol Dis. 43(2):346-355, 2011.

34 Gluck MR, Thomas RG, Davis KL, Haroutunian V. Implications for altered glutamate and GABA metabolism in the dorsolateral prefrontal cortex of aged schizophrenia patients. Am J Psychiatry. 159(7):1165-1173, 2002.

35 Huang Y, Zhao L, Jia B, Wu L, Li Y, Curthoys N, Zheng JC. Glutaminase dysregulation in HIV-1-infected human microglia mediates neurotoxicity: Relevant to HIV-1-associate neurocognitive disorders. J Neurosci. 31(42):15195-15204, 2011.

36 Werner P, Pitt D and Raine CS. Multiple sclerosis: Altered glutamate homeostasis in lesions correlates with oligodendrocyte and axonal damage. Ann Neurol. 50(2):169-180, 2001.

37 Zhao L, Huang Y, Tian C, Taylor L, Curthoys N, Wang Y, Vernon H, Zheng J. Interferon-α regulates glutaminase 1 promoter through STAT1 phosphorylation: Relevance to HIV-1 associated neurocognitive disorders. PLoS One. 7(3):e32995, 2012.

38 Lynch DS, Chelban V, Vandrovcova J, Pittman A, Wood NW, Houlden H. GLS loss of function causes autosomal recessive spastic ataxia and optic atrophy. Ann Clin Transl Neurol. 5(2):216-221, 2018.

39 Rumping L, Büttner B, Maier O, Rehmann H, Lequin M, Schlump JU, Schmitt B, Schiebergen-Bronkhorst B, Prinsen HCMT, Losa M, et al. Identification of a loss-of-function mutation in the context of glutaminase deficiency and neonatal epileptic encephalopathy. JAMA Neurol. 76(3):342-350, 2018.

40 van Kuilenburg ABP, Tarailo-Graovac M, Richmond PA, Drögemöller, MA, Pouladi R, Leen K, Brand-Arzamendi K, Dobritzsch D, Dolzhenko E, Eberle MA, et al. Glutaminase deficiency caused by short tandem repeat expansion in GLS. N Engl J Med. 30(15):1433-1441, 2019.

41 Rumping L, Tessadori F, Pouwels PJW, Vringer E, Wijnen JP, Bhogal AA, Savelberg SMC, Duran KJ, Bakkers MJG, Ramos RJJ, et al. GLS hyperactivity causes glutamate excess, infantile cataract and profound developmental delay. Hum Mol Genet. 28(1):96-104, 2018.

42 Häberle J, Görg B, Rutsch F, Schmidt E, Toutain A, Benoist JF, Belot A, Suc AL, Hohne W, Schliess, et al. Congenital glutamine deficiency with glutamine synthetase mutations. N Engl J Med. 353:1926-1933, 2005.

43 Spodenkiewicz M, Diez-Fernancez C, Rüfenacht V, Gemperle-Britschgi C, Häberle J. Minireview on glutamine synthetase deficiency, an ultra-rare inborn error of amino acid biosynthesis. Biology. 5(40):pii:E40, 2016.

44 Kapoor RR, Flanagan SE, Fulton P, Chakrapani A, Chadefaux B, Ben-Omran T, Banerjee I, Shield JP, Ellard S, Hussain K. Hyperinsulinism-hyperammonaemia syndrome: Novel mutations in the *GLUD1* gene and genotype-phenotype correlations. Eur J Endocrinol. 161:731-735, 2009.

45 Gulsuner S, Walsh, T, Watts AC, et al. Spatial and temporal mapping of de novo mutations in schizophrenia to a fetal prefrontal cortical network. Cell. 154(3):518-529, 2013.

46 Masson J, Darmon M, Conjard A, Chuhma N, Ropert N, Thoby-Brisson M, Foutz AS, Parrot S, Miller GM, Jorisch R, et al. Mice lacking brain/kidney phosphate-activated glutaminase (GLS1) have impaired glutamatergic synaptic transmission, altered breathing, disorganized goal-directed behavior and die shortly after birth. J Neurosci. 26(17):4660-4671, 2006.

47 Lek M, Karczewski KJ, Minikel EV, Samocha KE, Banks E, Fennell T, O'Donnell-Luria AH, Ware JS, Hill AJ, Cummings BB. Analysis of protein-coding genetic variation in 60,706 humans. Nature. 536(7617):285-291, 2016.
48 Zhu J, Djukovic D, Deng L, Gu H, Himmati F, Chiorean EG, Faftery D. Colorectal cancer detection using targeted serum metabolic profiling. J Proteome Res. 13(9):4120-4130, 2014.

49 Thomas SM, Kagan C, Pavlovic BJ, Burnett J, Patterson K, Pritchard JK, Gilad Y. Reprogramming LCLs to iPSCs results in recovery of donor-specific gene expression signature. PLoS Genet. 11(5):e1005216, 2015.

50 Zhu J, Djukovic D, Deng L, Gu H, Himmati F, Chiorean EG, Raftery D. Colorectal cancer detection using targeted serum metabolic profiling. J Proteome Res. 13(9):4120-4130, 2014.

51 Neale JH, Bzdega T, Wrobiewska B. N-Acetylaspartylglutamate: The most abundant neurotransmitter in the mammalian central nervous system. J Neurochem. 75(2):443-452, 2000.

52 Combs Jr GF. The vitamins: Fundamental aspects in nutrition and health (3rd ed.). Ithaca, NY: Elsevier Academic Press, 2008.

53 Thomson JA, Itskovitz-Eldor J, Shapiro SS, Waknitz MA, Swiergiel JJ, Marshall VS, Jones JM. Embryonic stem cell lines derived from human blastocysts. Science. 282(5391):1145-1147, 1998.
54 Agostini M, Romeo F, Inoue S, Niklison-Chirou MV, Elia AJ, Dinsdale D, Morone N, Knight RA, Mak TW, Melino G. Metabolic reprogramming during neuronal differentiation. Cell Death Differ. 23(9):1502-1514, 2016.

55 Albrecht J. Sonnewald U, Waagepetersen HS, Schousboe A. Glutamine in the central nervous system: Function and dysfunction. Front Biosci. 12:332-343, 2007.

56 Nonaka S, Hough CH, Chuang D-M. Chronic lithium treatment robustly protects neurons in the central nervous system against excitotoxicity by inhibiting N-methyl-D-aspartate receptor-mediated calcium influx. Proc Natl Acad Sci USA. 95:2642-2647, 1998.

57 Neale JH. N-Acetylaspartylglutamate (NAAG) IS an agonist at mGluR3 *in vivo* and *in vitro*. J Neurochem. 119(5):891-895, 2012.

58 Zuo D, Bzdega T, Olszewski RT, Moffett JR, Neale J. Effects of N-acetylaspartylglutamate (NAAG) peptidase inhibition on release of glutamate and dopamine in prefrontal cortex and nucleus accumbens in phencyclidine model of schizophrenia. J Biol Chem. 287(26):21773-21782, 2012.

59 Wang Y, Li Y, Zhao R, Lanoha B, Tong Z, Peer J, Liu J, Xiong H, Huang Y, Zheng J. Glutaminase C overexpression in the brain induces learning deficits, synaptic dysfunctions, and neuroinflammation in mice. Brain Behav Immun. 66:135-145, 2017.

60 Parent AS, Matagne V, Bourguignon JP. Control of puberty by excitatory amino acid neurotransmitters and its clinical implications. Endocrine. 28(3):281-286, 2005.
61 Terasawa E. Role of GABA in the mechanism and onset of puberty in non-human primates. Int Rev Neurobiol. 71:113-129, 2005.